Process Analytical Technology in Food Biotechnology

By means of sensors, signal processing, modelling and process control

Dissertation zur Erlangung des Doktorgrades

der Naturwissenschaften (Dr. rer. nat.)

Fakultät Naturwissenschaften

Universität Hohenheim

Institut für Lebensmittelwissenschaft und Biotechnologie

bei Prof. Dr. Bernd Hitzmann

vorgelegt von

Marc Stanke

geboren in Hannover

2017

Dekan Prof. Dr. Heinz Breer

1. berichtende Person: Prof. Dr. Bernd Hitzmann

2. berichtende Person: Prof. Dr.-Ing. habil. Jörg Hinrichs

Mündliche Prüfung am: 21.03.2018

Die vorliegende Arbeit wurde am _____ von der Fakultät Naturwissenschaften der Universität Hohenheim als „Dissertation zur Erlangung des Doktorgrades der Naturwissenschaften“ angenommen.

“Since all models are wrong the scientist cannot obtain a ‘correct’ one…yet he can derive results which match to a useful approximation, those found in the real world”

Georg Box 1979

Content

Chapter

1

Introduction and outline

Introduction

In August 2002, the Food and Drug Administration (FDA) announced a new initiative. The Pharmaceutical Current Good Manufacturing Practices (cGMP) for the 21st Century [1], which aims to improve pharmaceutical production as well as product quality. The aim of the initiative was to modernize the regulatory processes for medicine and biological products. To this end, the manufacturing industry is encouraged to use new technological advances and modern quality management techniques at an early stage. In addition, the assessment of new products and changes to existing processes should be carried out in a risk-based manner in order to focus the attention of the industry and the FDA on critical areas and thus to use the frequently limited resources effectively. Well documented and fully understood processes can be adapted more easily with an agile process. Otherwise it can be evaluated whether the changes are adapted in a well-understood area or in a critical field, which simplifies the estimation and facilitates the provision of additional data if necessary. In turn, the FDA also wants to do its part to ensure that their regulatory, audit and compliance guidelines are based on the state of the art science, as well as to improve the consistency and coordination of drug quality control programs. For this purpose, a number of multidisciplinary working groups have been set up, which are made up of FDA experts in various fields of scientific and regulatory practice within the FDA and are intended to advance the initiative's objectives. An important guiding principle of the initiative is the Science based regulation of product quality. Quality and productivity improvement have a common basis, reducing variability through process understanding. Producing companies have an interest to improve their productivity and the public health sector benefits from improved product quality and safety. The improved process understanding and the risk-based approach help the FDA to more efficiently perceive its regulatory role.

The guide to the implementation of the science based regulation of product quality is a framework for innovative pharmaceutical development, production and quality assurance. This is described in the regulatory framework Process Analytical Technology (PAT) for implementation [2]. The Process Analytical Technology Framework consists of a set of scientific principles and tools to promote innovation and a strategy for implementation. The strategy for implementation includes a PAT team of interdisciplinary experts from the FDA who carry out the process reviews and cGMP inspections, and a series of training, certifications carried out on the industry side and FDA side in collaboration. Conventional production of many products is carried out in batch processes, the quality of which is validated in the laboratory. However, the FDA's investigation within the framework of the cGMP for the 21st Century initiative has shown significant opportunities to improve the development, production and quality of many places by introducing innovative processes for development, process

analysis and process control. At the same time, the investigations have also shown that many companies are reluctant to use new systems. The reason that is often mentioned is an uncertainty as to the impact of the change on the regulatory process by the FDA as it is perceived as very rigid and unfavourable for innovation. It is precisely this point that the PAT initiative wants to adopt. The production of pharmaceutical products continues to develop with new scientific discoveries and technical innovations. The effective use of these new principles throughout the lifecycle of a product can both improve productivity and simplify the regulatory process. Therefore the PAT initiative wants to address this very precisely and make this possible. Product quality is to be controlled through an effective and efficient manufacturing process. The product specifications are based on a mechanistic understanding of how formulation and process factors influence the product. The risk-based regulatory approach takes into account the degree of scientific understanding as well as the factors influencing the product and the ability to reduce or prevent reduced product quality through appropriate control strategies. A process counts as fully understood when all sources for the process variability are identified and understood and these are represented in the process. In addition, the product quality must be predictable accurately and reliably for all materials, processes and production parameters as well as environmental variables. This is necessary even though the analytical methods to determine the initial materials are very precise, many physical or mechanical attributes are not necessarily well understood. Consequently fluctuations in the initial situation will be reflected in the quality of the final product.

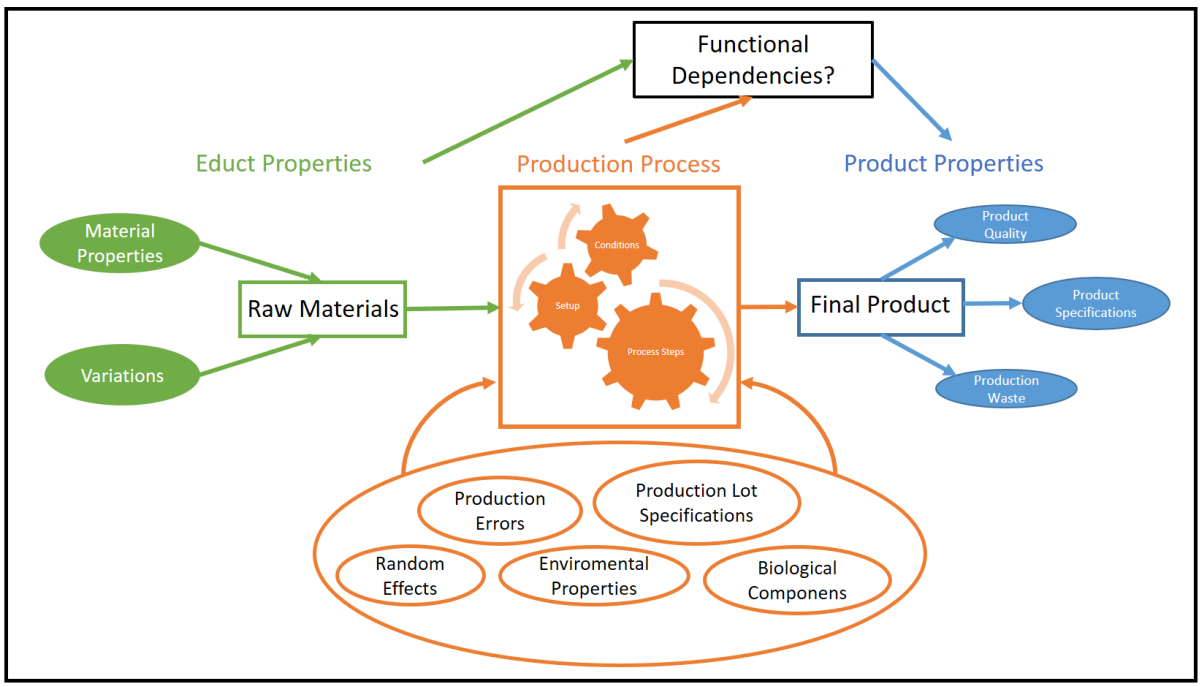

Figure 1: Production flow chart, possible disturbance values and important properties of the final product found in typical food and drug production processes. The functional dependencies between the raw material, the production process and the properties of the final product are a key aspect of the PAT initiative.

The PAT Framework defines four possible tool categories. The field of (bio)informatics is a key player in the PAT framework to provide the necessary algorithms and software to implement the various tools. They allow scientists and producers to evaluate complex relations and do extensive calculations to interpret experiments and production processes.

Process and endpoint monitoring and control tools

With increasing computational power and improving miniaturization, the evaluation of measurements became available almost instantaneous for all sensor technology. This leads to the possibility of on-/ at- and in-line process parameter monitoring and data generation. This data can further be used to control the processes. Although in recent years many contributions have been published dealing with closed loop control, only a minority was actually applied in real bioprocesses. A review on this close loop control strategies is given by Stanke and Hitzmann [3]. In any case a control algorithm, capable of interpreting the input values is needed, which intelligently and reliably decides on the control action that needs to be taken. Process knowledge can be obtained studying the process itself, but to study the process an appropriate measurement system is needed. The measurement system must provide all necessary information needed to completely understand a process. This can be obtained via direct measurements which will give the best knowledge about a desired process value. Or in case of an indirect measurement via for example a soft sensor design. These are summarized in the following category.

Modern process analysers or process analytical chemistry tools

*I*n biotechnology and food technology processes are often employing a biological component for their production which is especially affected by variations. Analytics and science in food production is facing complicated physical matrices of heterogeneous molecules. The main components in the food sector are due to their nutritional value various kinds of fats, proteins and carbohydrates. These are incorporated in matrices of very different states e.g. gels, foams with varying pore sizes and even as biological components. To ensure the desired product quality with reasonable financial investment is the given challenge. Two very specific approaches are given by Stanke et al. [4], presenting a very sensitive on-line capable sensor for process monitoring. Here the unspecific quantity “sonic velocity” is calculated, measuring resonance phenomena. Stanke et al. [5] are further presenting a theoretical model applied on actual measurements to predict important proofing parameters, introducing a soft-sensor design for this specific process. More general approaches are metabolic engineering witch is trying to generate knowledge for e.g. biopharmaceutical and food engineering processes to improve the understanding of up-scaling processes as well as the influence of raw materials and varying process conditions. [6-8] The recent challenges for bioinformatics emerging from the vast amount of

data generated by personalized medicine is summed up in a review by G. H. Fernald et al. [9]. The translational bioinformatics and the system biology both try to extract knowledge from data. Dynamic mechanistic models as well as data driven models are fueled by the vast amount of available data. Many studies try to improve the amount of information that can be extracted from large unstructured datasets (NoSQL Databases) as well as generating mechanistic and data driven models. Also handling big data in bioinformatics is the field of translational Bioinformatics emerging from the high throughput methods which became a key component in e.g. biomedical research. Examples for translational approaches can be found at J.D. Tenenbaum [10] and Y. Vodovitz and G.An [11]. Prior to the recent developed process analysers are potent tools for data acquisition and analysis summarized in the following category:

Multivariate data acquisition and analysis tools

To keep the degree of automation high and dynamically react to changes in the process the feature selection of a measurement (e.g. peak detection) becomes important in many applications. Over the years many approaches in the field of machine learning as well as data mining and specialised applications have been introduced. A review and forecast of upcoming applications can be found at Y. Saeys et al. [12].

Continuous improvement and knowledge management tools

With higher computerization and the availability of vast amounts of data new challenges emerge. New skill sets in the field of bioinformatics are needed to guarantee high quality data as well as the validation of the developed tools. Processes need to be standardized to help a safely introduction and effective use of new applications. A review on the current fields of regulatory bioinformatics can be found at M.J. Healy et al. [13].

Since a higher degree of automation is the general purpose of the PAT initiative, all tools are aiming to provide the needed information for a successful realization. In the last progress report from December 2014 [14] the formation of various internal committees and research teams is described. The FDA is building up its internal teams in regards of PAT and provides trainings, conferences, several workshops and collaborative research on PAT applications with major pharmaceutical companies. Despite all the effort of the FDA and various publications regarding PAT applications and tools there is still a long way to go.

References

[1] US Food and Drug Administration (2004), Pharmaceutical cGMP for the 21st century: a risk based approach, FDA Rockville.

[2] US Food and Drug Administration (2004) PAT guidance for industry – a framework for innovative pharmaceutical development, manufacturing and quality assurance, FDA Rockville.

[3] M. Stanke and B. Hitzmann (2013), Automatic Control of Bioprocesses, Measurement, Monitoring, Modelling and Control of Bioprocesses. C.-F. Mandenius and N. J. Titchener-Hooker, Springer Berlin Heidelberg. 132: 35-63.

[4] M. Stanke, P. Lindner, S. Holz, B. Hitzmann (2013), Automated sonic velocity calculation based on ultrasonic resonator measurements for on-line process monitoring, Sensors and Actuators A: Physical, 198: 69-74.

[5] M. Stanke, V. Zettel, S. Schütze, B. Hitzmann (2014), Measurement and mathematical modeling of the relative volume of wheat dough during proofing, Journal of Food Engineering, 131: 58-64

[6] S. S. Fong (2014), Computational approaches to metabolic engineering utilizing systems biology and synthetic biology, Computational and Structural Biotechnology Journal, Volume 11, Issue 18, Pages 28-34.

[7] M. Meisner and D. M. Reif (2015), Computational Methods Used in Systems Biology, In Systems Biology in Toxicology and Environmental Health, Academic Press, Boston, Pages 85-115

[8] M. Sato, S. Matsuoka, P. M. Sloot, G. D. van Albada, J. Dongarra, M. Cannataro, R. Weber dos Santos, J. Sundnes (2011), Biomedical and Bioinformatics Challenges to Computer Science: Bioinformatics, Modeling of Biomedical Systems and Clinical Applications, Procedia Computer Science, Volume 4, Pages 1058-1061.

[9] G. H. Fernald, E. Capriotti, R. Daneshjou, K. J. Karczewski and R. B. Altman (2011), Bioinformatics challenges for personalized medicine, Bioinformatics, Vol. 27 no. 13, Pages 1741–1748.

[10] J. D. Tenenbaum (2016), Translational Bioinformatics: Past, Present, and Future, Genomics, Proteomics & Bioinformatics, Volume 14, Issue 1, Pages 31-41

[11] Y. Vodovotz and G. An (2015), From Data to Knowledge in Translational Systems Biology: An Overview of Computational Approaches Across the Scientific Cycle, In Translational Systems Biology, Academic Press, Pages 81-88

[12] Y. Saeys, I. Inza, P. Larrañaga (2007) A review of feature selection techniques in bioinformatics. Bioinformatics. 23(19):2507-17.

[13] M. J. Healy, W. Tong, S. Ostroff, H.G. Eichler, A. Patak, M. Neuspiel, H. Deluyker, W. Slikker Jr. (2016), Regulatory bioinformatics for food and drug safety, Regulatory Toxicology and Pharmacology.

[14] US Food and Drug Administration (2014), Progress Report on Process Analytical Technology, FDA Rockville.

Outline

The work in this thesis focuses on the development and understanding of algorithms and software solutions for the implementation of PAT tools. To separate the work from mere theoretical concepts all the developed software underwent proof of principle measurements, hence demonstrating applicability.

Chapter 2 "**Automatic control of bioprocesses**" will give a review on process control tools for biotechnological processes of the last seven years. New control strategies and sensor developments employed for process control in actual processes will be presented.

Chapter 3 "Automated sonic velocity calculation based on ultrasonic resonator measurements for on-line process monitoring" is presenting a very sensitive on-line capable sensor for process monitoring. Here the unspecific quantity "sonic velocity" is calculated measuring resonance phenomena. The chapter is focusing on the optimal evaluation of the raw signals and is presenting measurements on pure water to demonstrate the high accuracy and precision.

Chapter 4 "Measurement and mathematical modeling of the relative volume of wheat dough during proofing" is presenting a theoretical model applied on actual measurements to predict important proofing parameters. This soft sensor design (process analyzer) is used to obtain the specific CO_2 production rate of a microorganism, number of incorporated bubbles and viscosity for this very specialized biotechnological process.

Chapter 5 "Summary and final remarks" will sum up the findings of the previous chapters and link them in the context of the PAT tools.

Chapter

2

Automatic control of bioprocesses

M. Stanke and B. Hitzmann (2013),

Measurement, Monitoring, Modelling and Control of Bioprocesses. C.-F. Mandenius and N. J. Titchener-Hooker, Springer Berlin Heidelberg. 132: 35-63.

Abstract

In this contribution different approaches for open loop and closed loop control applied in bioprocess automation are discussed. Although in recent years many contributions have been published dealing with closed loop control, only a minority was actually applied in real bioprocesses. Due to the immense variety of bioprocesses and increasing demands single approaches for a control suggestion are found more rarely. Most publications are combining closed loop control techniques to construct hybrid systems. These systems are supposed to combine the advantages of each approach to a well performing control strategy. The majority of applications are Soft-sensors in combination with a PID controller. The reason that soft-sensors got this importance for control purposes demonstrate the lack of direct measurements or its big additional expenditure for robust and reliable on-line measurement systems. On this account some applications are proposed to control fermentations either at their oxidative maximal capacity like the probing feeding approach or the control based on the metabolic state tolerating small amounts of overflow metabolism. Increasing fields are also model predictive controller. However reliable and robust process models are required as well as very powerful computers to provide the computational demand. The lack of theoretical bioprocess models is compensated by hybrid systems combining theoretical models, fuzzy logic and/or artificial neural networks methodology. Although many authors suggest a possible transfer of their presented control application to other bioprocesses, the algorithms are mostly specialized to a certain organisms or certain cultivation condition as well as to a specific measurement system

Keywords: Closed loop control, PAT, fermentation, bioprocess, review

Content

Abbreviations and nomenclature

Symbol	Name
ANN	Artificial neural network
CER	Carbon dioxide evolution rate
C_{feed}	Substrate concentration in feed flow
$C_{O2,feed}$	Oxygen concentration in gassing flow
CPR	Carbon dioxide production rate
DO	Dissolved oxygen

E	Ethanol
e(t)	Control deviation at time t
EKF	Extended Kalman filter
FIA	Flow Injection analysis
GC	Gas chromatography
HCDC	High cell density cultivation
HPLC	High pressure liquid chromatography
K	PID controller parameter matrix
k_1,k_2,k_3	Kinetic parameters
K_d	PID controller parameter derivative part
K_i	PID controller parameter integral part
K_La	Oxygen transfer coefficiant
K_p	PID controller parameter proportional part
K_S	Kinetic constant for substrate consumption
LLM	Local linear model
LoLiMoT	Local linear model tree
m	Substrate consumption due to the cell maintenance
MIMO	Multiple input multiple output
MISO	Multiple input single output
MPC	Model predictive controller
NMPC	Non-linear model predictive controller
ORP	Oxidation-reduction potential
OTR	Oxygen transfer rate
OUR	Oxygen uptake rate
PID	Proportional, integral, derivative
r_{DO}	specific oxygen consumption rate
$r_{DO}X_t$	oxygen consumption rate
S	Substrate
S_{crit}	Critical substrate value (overflow metabolite formation)
SISO	Single input single output
t	Time
u(t)	Control action at time t
V	Cultivation volume
V_0	Initial volume

V	Substrate feeding flow
X	Biomass
$x(t),x$	Input values (measurement)
X_0	Initial biomass
Y_{XS}	Yield factor biomass formation
μ	Specific growth rate
$\mu_B(X)$	Membership function of a fuzzy logic controller
μ_{crit}	Beginning of overflow metabolism
μ_{max}	Maximal specific growth rate
μ_{sp}	Set-point of specific growth rate
Y_{XS}	Yield factor biomass formation
τ	Integration variable

1 Introduction

Due to competition the industry tends to increase the degree of automation in production processes. Only an automated system is never tired, always attentive and will act reliable and therefore can provide an optimal process operation. It can react fast to changes in the raw material's quality as well as changes in environmental conditions. As a result the energy and material input can be decreased and the process safety, the product yield and quality can be increased. This applies, of course, also for bioprocesses. The operation of these processes is usually carried out in three successive steps:

Up streaming (filing, sterilization, mixing)

Cultivation / enzyme reaction (growth of cells, bioconversion and production)

Down streaming (harvesting, separation, concentrating and crystallization)

Each step demands a high degree of automation. In the first step standard automatic sequence control units are available. The quality of raw materials is of special importance for the subsequent steps. The automation in the second step is more complicated since complex transport processes are combined with a multitude of dynamic biochemical reactions during the cultivation. Therefore, one has to deal with a complex, non-linear, multi parameter, time variant system. Little detailed comprehensive knowledge is available. The microorganisms used for the synthesis of the product have many inherent closed loop systems on their own, which can only be manipulated indirectly through environmental conditions by physical and chemical variables. Frequently open loop control systems are employed to control cultivation processes. In order to realize a closed loop control system reliable measurements are vital. However, the application of closed loop control is still rare, due to many reasons:

In many cases important process variables can only be determined on-line with excessive effort. They become available delayed by a dead time as well as lag elements and also discontinuous. Most of the bioprocesses are batch or fed-batch processes; therefore one has to deal with a transient (not stationary) process, where the automation task is to provide an optimal environment for the microorganism. The typical goals of automation of bioprocesses are to

- compensate failure of any kind
- minimize energy and raw materials
- maximize yield and product quality
- guarantee a safe operation
- prevent substrate, overflow metabolite or product inhibition

- ensure a well-directed induction and repression of enzyme production
- prevent high shear stress
- present an optimal environment for the organism for growth as well as production

With the help of standard control algorithms some of these goals can already be achieved. Basic bioreactor equipment often includes control algorithms for the volume, temperature, pH, dissolved oxygen, and addition of antifoam agents. However these basic controllers are not always sufficient for special application.

In this contribution the state of the art bioprocess automation and recent progress will be discussed. An overview of the discussed application is presented in Table 3.1.

2 Controller design

2.1. Direct measurements

Especially for closed loop control purposes measurements are fundamental. For bioprocesses in-situ measurements like temperature, pH, dissolved oxygen concentration (DO), optical density, pressure and at line measurements like the exhaust gas composition are performed most frequently and can be used as input variables for a controller [1,2]. At-line measurements based on spectrophotometric , mass spectrometric, HPLC, GC and flow injection analysis system (FIA-systems) are applied less frequently for on-line measurements and even less often as input variables for a controller [1-3]. Due to the fact that direct measurements of important variables, such as growth rate, substrate uptake rate and carbon dioxide production rate are missing, soft-sensors have been established which are a kind of indirect measurements that can provide an access to relevant variables using different techniques.

2.2 Soft-sensors

Economist and business consultant Peter Drucker once said: “If you can’t measure it, you can’t manage it”. Although he didn’t mean bioprocesses, it can also be applied here. Keeping that in mind, soft-sensors will here be introduced to “manage the immeasurable”. Soft-sensors or virtual sensors are employed to calculate variables out of one or more of the directly measured variables. Commonly employed indirect measurements based on theoretical models are oxygen uptake rate (OUR), oxygen transfer rate (OTR), carbon dioxide production rate (CPR) and the respiration coefficient, which are calculated from exhaust gas measurements and the aeration rate. The

identification of critical needs to successfully develop state of the art soft-sensors is presented by R. Luttmann et al. [4]. They particularly discuss soft-sensor methods for bioprocess engineering and pharmaceutical applications.

Data-driven soft-sensors are using chemometric models for the estimation of process variables [2,3,5]. An example is the calculation of the glucose concentration and dry cell mass concentration out of fluorescence data [6]. Using these data driven approaches one has to be attentive not to leave the calibration range. Therefore theoretical model-based soft-sensors have usually a more broad application range. An important class of these soft-sensors is based on state-observers.

2.2.1 State observer

A state-observer uses a dynamic theoretical model (state model) of the process to estimate process variables (state variables). Using available measurements the state observer corrects the estimated state variable in such a way, that its values will converge to the true process values. For the implementation of a state observer detailed knowledge of the process is necessary. The advantage of state-observers is the determination of immeasurable process variables which can be used for process automation.

An example is given by Jenzsch et al. [7]. They estimated the biomass out of a mass-balance-based state-observer employing the relation between OUR, CPR and base consumption. One kind of standard state-observers are the Luenberger observer [8] and the Kalman filter. A special class of Kalman filter will be discussed in the next chapter.

2.2.2 Extended Kalman filter

To smooth noisy measurement signals as well as to estimate non measurable process variables, different Kalman filters have been applied for controller implementation. For this purpose process knowledge is required in the form of a dynamic state model, a measurement model and known measurement noise. The main idea of the Kalman filter [9] is the minimization of the error covariance of the state variables estimation. Therefore not only the process model, but also the estimated error covariance differential equations have to be integrated on-line. If a non-linear state model is used, the filter is called extended Kalman filter (EKF). A continuous-discrete EKF uses a continuous non-linear state model and a discrete measurement model. The differential equations are integrated as long as no new measurement value is available. If a new measurement is available, the filter equation is applied. As a result the estimation error covariance is minimized and the estimated

values of the state variables are adjusted to the measurements. By using a Kalman filter, the time varying characteristics of cultivation processes can be implemented in a control algorithm.

A general overview of specialized state observers is given by Kawohl et al. [10] who compared different optimization-based state estimation algorithms in order to judge their estimation quality. The Bayesian maximum, a posteriori based constrained extended Kalman filter, the moving-horizon-state-estimation and the classical unconstrained extended Kalman filter are compared during Monte Carlo simulation experiments. The authors conclude that the moving-horizon-state-estimation shows higher potential for state estimation in small systems. For higher order systems the adjustments of the filter parameters as well as the numerical optimizations were more difficult.

2.3 Control action

The control action (actuating variable) is the resulting action the controller performs corresponding to the control law, e.g. setting substrate flow rate to the appropriate value. Figure 2.3.1 shows the principle of a closed loop controller. The control action is the result of the feedback given by the process measurement, which might be further processed by a soft-sensor, and the control algorithm. The overall goal is to minimize the deviation between the set-point and the controlled variable.

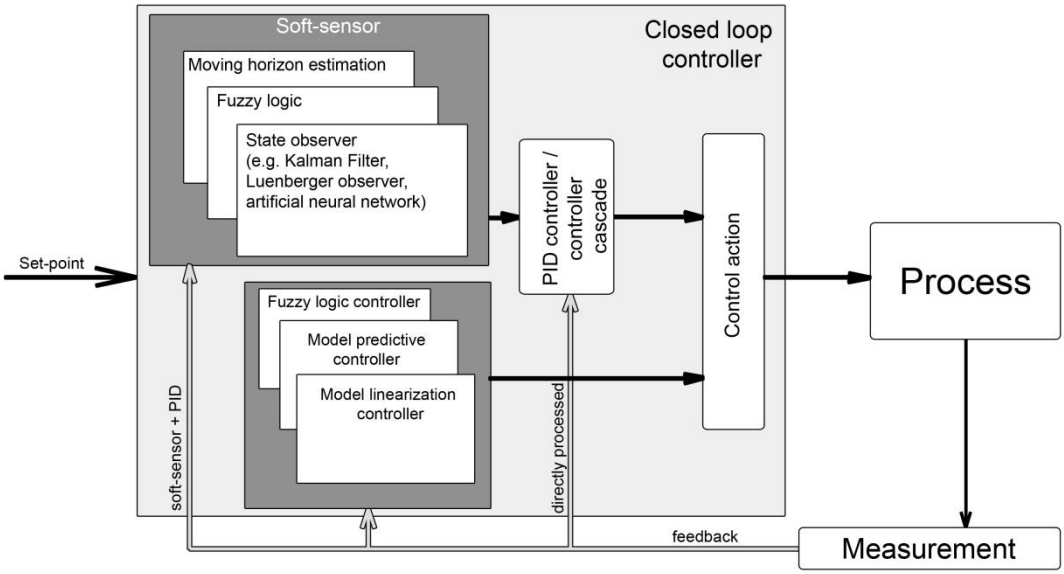

Figure 2.3.1 A general schematic of different (alternative) closed loop control schemes

The following chapters will discuss a wide variety of applications of state of the art control applications for bioprocess automation. First, PID-based controllers in combination with different soft-sensors will be presented and after that model linearization approaches are discussed. This is followed by fuzzy logic and artificial neural network-based controller, model predictive controller as

well as combinations of the three latter methods. Lastly probing feeding, extremum seeking control and a heuristic control strategy will be discussed.

A very basic approach is presented by Lindgren et. al. [11] and Kriz et al. [12] based on a real time in situ SIRE® biosensor system combined with an two-step controller (on-off control) for yeast cultivations at different biomass concentrations. Their controller could manage a set-point of 10 mM glucose for 60 min with a standard deviation of 0.99 mM at biomass concentration up to 80 gL^{-1}.

3 State of the art control algorithm

The most common closed loop control algorithm is the PID controller. Here e(t) the difference between the controlled variable and the set-point at the time t is used to calculate the control action. Equation (2.1) is the general form of a PID controller, with K_p as proportional gain, K_i the integral gain, K_d the derivative gain parameter and u(t) as control action.

$$u(t) = K_p e(t) + K_i \int_0^t e(\tau)d\tau + K_d \frac{d}{dt} e(t) \tag{3.1}$$

The basic PID control is an algorithm responding to current changes with constant parameters, in which the knowledge of the process is presented. A special form of the PID controller is the PI controller which is lacking the derivative part K_d=0 leading to a more steady system against noisy measurement data. This type of controller can be found most frequently.

3.1 Open loop – closed loop controller

The simplest control action for a cultivation process is an open loop control. One can rearrange typical mass balance equations describing a cultivation process in a stirred tank reactor to obtain e.g. equation (3.2), representing the feeding law of substrate. This is basically an assumption of a known constant substrate consumption rate as well as a predetermined constant specific growth rate μ_{sp}, which is smaller than the maximal specific growth rate.

$$F_0(t) = \left(\frac{\mu_{sp}}{Y_{XS}} + m\right) \frac{V_0 X_0}{C_{feed}} e^{\mu_{sp}(t-t_0)} \tag{3.2}$$

$$X_0 = X(t=0) \qquad V_0 = V(t=0)$$

Using such a controller the cultivation feed is performed following a predefined trajectory. The knowledge of the inoculum size as well as the specific growth rate and the yield factors are obviously needed to perform this kind of open loop control which is called feed-forward control. Advantages and disadvantages of open loop control are presented by Gnoth et al. [13]. In case of disturbances

(e.g. wrong pH value in consequence of a failure) the system's behavior is going to differ from the prediction. In this case the feed is predicted incorrectly and the result of the cultivation is not as designated, resulting in a waste of resources. To prevent this, the plainest closed loop control approach is to add a feedback to the feed-forward term for regulatory action. These feed-forward / feedback controllers are usually a class of single input single output (SISO) controller. The control law equation (3.4) is the sum of the feed-forward part F_0 which is the estimation of the approximately needed feed rate equation (3.2) at time t and the feedback part F_b, in this case delivered by a PI algorithm equation (3.3).

$$F_b(t) = K_P e(t) + K_i \int_0^t e(\tau) d\tau \tag{3.3}$$

$$u(t) = F_b(t) + F_0(t) \tag{3.4}$$

3.2 PID control based on soft-sensors measurements

Controller with more than one input value are classified as multiple input single output (MISO) or multiple input multiple output (MIMO) and are represented as multi-loop PID controller or cascade PI controller. MIMO systems are coupling their input values according to the interaction and are therefore able to map higher complexities of the controlled process. They are supposed to be more accurate in their control action than SISO systems. The structures of both controllers (SISO and MIMO) are shown in Figure 3.2.1.

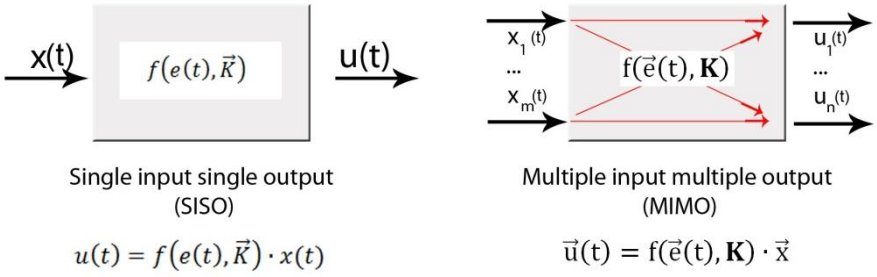

Figure 3.2.1: The scheme of a SISO controller compared with a MIMO controller

Applications of these controller types for bioprocess automation will be discussed in the following sections.

3.2.1 Single input single output control

A combination of a Kalman filter, which measurements came from a glucose FIA system and a PI controller, are presented by Arndt and Hitzmann [14]. The system was applied for *a S. cerevisiae* cultivation to control the glucose concentration. The Kalman filter estimates the glucose and biomass concentration, the volume of culture broth and the maximal specific growth rate. The predicted values were used for a PI feedback controller with set-points of 0.08 gL^{-1} and 0.05 gL^{-1}. The controller established well defined growth conditions over several hours. The authors demonstrated that in contrast to the higher set-point, no ethanol was produced at the lower set-point. A similar approach was applied by Arndt et al. [15] for an *E. coli* cultivation to produce phytase. They discussed the response of the controller during a failure of the glucose FIA measurement. After the process analyser was fixed, the on-line glucose measurement returned after 0.2 h to the set-point of 0.2 gL^{-1} and in total of 0.4 h to the intended performance. Control strategies based on DO set-points between 5 and 10 % did not result in a higher yield of phytase as shown by Kleist et al. [16].

A set-point substrate controller of glucose concentration for baker yeast fermentation was presented by Klockow et al. [17]. They compensated the dead time of 6 min. caused by the FIA measurement system using an extended Kalman filter in combination with a ring buffer, where the estimated variables as well as the pumping rate are stored. If a new measurement value from the FIA system is sent to the Kalman filter the dead time is considered by taking the historic process variable data of that time point out of the ring buffer and the ordinary filtering is carried out followed by the simulation up to the current time. Since during the control phase the relative standard deviation of the measured values and the set-point were 2.9 % and 4.4 % for the set-point of 0.07 gL^{-1} and 0.5 gL^{-1} respectively, the authors concluded that the control was successful.

Roever and Slavov [18,19] presented a closed loop control for the application of an *E. coli* cultivation. They also used the measurements from a glucose FIA system for a substrate control of the bioprocess. They tested three different approaches by using the FIA measurements with a PI controller, the measurements processed by an EKF and a PI controller as well as the measurements processed by an EKF combined with a Smith predictor and a PI controller. The latter was used to compensate the dead time of the FIA measurements. The authors claim a satisfactory control of the glucose concentration and emphasize the superiority of the control employing an EKF resulting in higher biomass yields.

3.2.2 Multiple input single/multiple output control

Wahab et al. [20] applied a multiple input single output controller for the DO and nitrate control in Waste Water Treatment process (WWT). They carried out extensive simulation studies on a non-linear model to demonstrate the superior performance concerning set-point tracking and disturbance robustness.

Another MISO approach is given by Jenzsch et al. [7] presenting a non-linear adaptive controller based on multiple input (oxygen uptake rate, carbon dioxide production rate and base consumption) to estimate the specific growth rate. They are comparing the results of their generic model control to the control performance employing only a PI controller. The generic model control shows better performance due to the model based feed-forward part and on-line adjusted control parameters obtained out of the state estimation.

Cascade PI/PID controller are employed and used to increase the precision of the PI principle mostly for non-linear control problems. Typically a so called slave control loop (inner control loop) is nested into a master control loop (outer control loop) as can be seen in Figure 3.2.2.

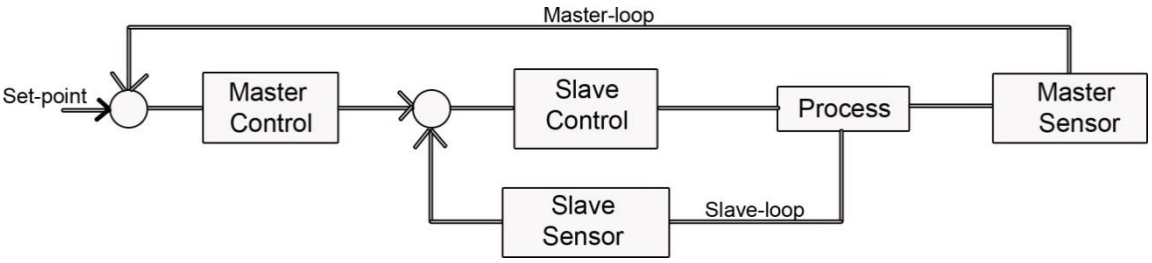

Figure 3.2.2 Scheme of a cascade process control system

Biener et al. [21] are using this principle to precisely control the temperature in the reactor considering a controller cascade for the reactor jacket and the reactor inside. The temperature inside the reactor is the main purpose of this control. Therefore it is the outer cascade circle that is called *master-loop*. The temperature of the reactor jacket is used for the inner *slave-loop.* The state observer for process control is using a heat balance equation that calculates the specific growth rate out of the heat flow that is meant to be evoked by the cell metabolisms. Based on the specific growth rate estimation they formulate a control law for the substrate feed rate. This controller design is employed on a high cell density cultivation (HCDC) of *E.coli* producing green fluorescence protein. The authors suggested that the method is advantageous for HCDC because of the high heat flow due to the high cell density and describe a gain of sensitivity with increasing biomass. The specific growth

rate can be controlled just below the critical growth rate where overflow metabolites occur. The authors demonstrate that no other measurement is necessary except DO concentration to guarantee an aerobic milieu. The determination of the heat flow generated by the cells and therefore the specific growth rate can be estimated reliably. Since the method is only using easy and fast measurable process variables, they suggest a potential for its application in standard industrial bioprocesses. They recently applied the described method to a *Saccharomyces cerevisiae* cultivation [22] showing the transfer of the technique to another organism. However, this method is applied to standard cell growth in 15 L and 30 L reactors. The method is not applicable after e.g. product induction, due to the changing heat balance while the cells change their metabolism.

Soons et al. [23] applied the cascade principle to precisely control the dissolved oxygen using the oxygen in the reactor headspace (*slave-loop*) and the dissolved oxygen in the medium (*master-loop*). They employ a closed loop control based on the DO concentration. With the simplification that the oxygen uptake rate is proportional to the OTR, the specific growth rate of the cultivation can be held at a constant level by controlling the DO concentration. This is shown in equation (3.5). According to Figure 3.2.2 the closed loop control of the dissolved oxygen is carried out through the cascade control. The outer loop equation (3.7) is comparing the measured DO (DO_{sensor}) with the set-point. The result is handed to the inner loop equation (3.8), calculating the controller output through the difference between headspace and medium.

$$OUR = OTR = k_L a\left(O_{2,head} - DO\right) \tag{3.5}$$

$$\frac{dO_{2,head}}{dt} = \frac{F_{O_2}}{V_{head}}\left(O_{2,in} - O_{2,head}\right) - OTR \tag{3.6}$$

$$O_{2,a} = K_p(DO_{set} - DO(t)_{sensor}) + K_i \int_0^t (DO_{set} - DO(\tau)_{sensor})d\tau \tag{3.7}$$

$$O_{2,in} = K_p\left(O(t)_{2,a} - O(t)_{2,head}\right) + K_i \int_0^t \left(O(\tau)_{2,a} - O(\tau)_{2,head}\right)d\tau \tag{3.8}$$

The cascade is realized by using the result of the PI control action of equation (3.7) in the control action of equation (3.8). It provides a more flexible and sophisticated control as if only one PI controller would be employed because not only the transport of oxygen between the gassing flow and the medium is considered, but also the transport from the headspace of the reactor into the medium. Further, Soons et al. are using a Kalman filter calculating the specific growth rate from the oxygen consumption provided from the DO control cascade. They demonstrated the implementation of a stable and robust closed loop controller for specific growth rate control. The method does not need an on-line model and lacks therefore a complex implementation. They show through simulations and feed batch experiments, that the controller is robust against disturbances and able

to maintain the specific growth rate of vaccine producing *Bordetella pertussis* at a constant level of □=0.05 h^{-1}.

Bodizs et al [24] observed that simple PI controllers for DO does not perform well enough in their system and therefore employed a cascade controller. Since they implement the controller to an established reactor, they used a set of available multiple inputs, namely OUR, CPR, DO and volume. The process is a 2,700 L fed-batch filamentous fungal fermentation. The control is applied to substitute a predetermined feeding strategy that is employed to guarantee no limitation of oxygen. The dissolved oxygen consumption rate $r_{DO}X_t$ is measured via a soft-sensor using the approximation of equation (3.9), whereas β is a proportionality factor and CER is the carbon dioxide evolution rate, which is assumed to be approximately the carbon dioxide transfer rate.

$$r_{DO}X_t = \beta \frac{OUR+CER}{V} \tag{3.9}$$

The *master-loop* is controlling the specific consumption rate r_{DO}. The *slave loop* controller is applied to control the feed rate based on OUR and CPR measurements. It is possible to efficiently control the specific consumption rate of oxygen. The main advantage is that it is not limited to a specific strain of microorganisms and applicable for a wide variety of fungal fermentations.

Another application for MIMO-PID bioprocess control is a multi-loop PID feedback controller for HCDC control applied by Chung et al. [25], coupling the OTR and the CPR. They are comparing the method to a model predictive controller and presented better results for their MIMO-PID using simulation studies. The controller can compensate disturbances in the measurement data for exhaust gas. Ranjan and Gomes [26] are also applying a cascade MIMO showing the performance enhancement against a normal PI controller.

For all these previously described applications the parameters of the PID controller must be determined. Different approaches to determine the PID parameters will be discussed in the next chapter.

3.2.3 PID Tuning

The obviously crucial part for all PID control based approaches is the determination of the corresponding PID parameter values. Changes in the process dynamic will most likely lead to suboptimal control actions. Ideally tuned controller should show a minimum of oscillation and lead the system fast and reliable to the set-point.

The tuning methods are divided into two groups: the parametric model methods tuning approaches and non-parametric. The parametric methods are using either model or experimental data to determine the controller parameters and are mostly described as off-line tuning methods, though also on-line approaches are tested. The non-parametric methods only partially use models like critical states and are suitable for on-line use as well as for an implementation without previous extensive plant studies. Wahab et al. [20] are comparing four non-parametric methods for multivariable PID tuning introducing one on their own and comparing it with the established methods from Davison [27], Penttinen–Koivo [28] and Maciejowski [29]. Soons et al. [23] are using a parametric tuning algorithm proposed by Bastin and Dochain [30] guaranteeing a stable behavior and a fast convergence towards the set-point. Other parametric approaches to tune a PID controller are described in many publications [19,20,31-33] where the authors are using e.g. genetic algorithms to obtain the optimal parameters.

The on-line estimation of the control parameters is described by Bastin and Dochain [30] as well as by Perrier et al. [34]. This is used in various control strategies [35-38], where the upper bound of the estimation error is minimized on-line and the resulting parameters are considered to be the optimal ones. Another approach in this direction is given by Kansha et al. [39] introducing a self-tuning PID design applying just-in-time learning. This algorithm is comparing a given database to the state of the process on-line and adjusts the gain parameter according to the obtained results and performs a self-tuning that is derived from the Lyapunov method [40] to guarantee a convergence of the given gain parameters.

3.3 Model linearization based control

Due to the inherent complexity, non-linearity and non-stationarity of the bioprocess Renard et al. [41] propose a so called RTS control scheme with Youla parameterization to overcome the bioprocess problems. They are developing their control approach for a *S. cerevisiae* cultivation controlling the ethanol concentration on a non-zero value. For substrate concentrations higher than the critical substrate concentration S_{crit} the occurrence of overflow metabolism is assumed. Since S_{crit} for yeast fermentations is at 0.1 gL^{-1} the authors suggest respiro-fermentative conditions and a quasi-steady state of the substrate concentration (considering no accumulation of substrate and instantaneous consumption, as long as the process does not deviate dramatically from the predetermined operation conditions). They get the following model for the relation between feed F_{in} and the measured ethanol concentration as well as the discrete time transfer function, respectively,

which are shown in the equations (3.10) – (3.13) (Here we are neglecting a few simplifications to keep the introduction of the model as simple as possible).

$$\frac{dE}{dt} = \frac{k_1 S_{in} - E}{V}\left(\dot{V} - d_x(t)\right) \tag{3.10}$$

$$d_x(t) = \frac{k_2 r_1}{k_2 \dot{V} - E} V_0 X_0 e^{(\mu \cdot t)} \tag{3.11}$$

$$r_1 = min(\mu_s, \mu_{crit}) \tag{3.12}$$

$$\mu = \mu_{max} \frac{S}{S + K_S} \quad with \quad \mu_{crit} = \mu_{max} \frac{S_{crit}}{S_{crit} + K_S} \tag{3.13}$$

Derived from equation (3.11) they get a time discrete transfer function that maps the feeding rate to the ethanol concentration, which is linearized for the purpose of control law application. The controller is considering the cell growth as an unstable exponential disturbance. The control method is only based on the on-line measurement of ethanol. For the yield coefficient a rough estimation (e.g. from literature) seems sufficient. They identify the state between fermentative and respirative operation as another way to control the specific growth rate close to the critical value where overflow metabolism occurs. They initially employ the controller to a laboratory scale fermentation [41] with a set-point of 0.7 g L^{-1} ethanol concentration with very small errors in the controlled variable. Later in the cultivation they observe an accumulation of ethanol, considering the limitation of oxygen. This is considered in a subsequent investigation [42] leading to a redesign in the controller scheme employing a feed-forward term and determination of the OTR from the exhaust gas measurements. The performance of the new proposed controller is evaluated via simulation studies of the process with off-line data. The same control algorithm was later [43] employed in an industrial fermentation process. The authors are claiming an increased productivity of 40 % using their algorithm compared to the up to then used open-loop control.

Cannizzaro et al. [44] and Valentinotti et al. [45] are describing a linearization approach capturing the main macroscopic processes, exponential substrate uptake and very small production of ethanol for laboratory scale. They suggest it as another way to control the specific growth rate close to the critical value where overflow metabolism occurs. They maintain the overflow metabolite concentration (ethanol and acetate for yeast and *E. coli*, respectively) and view the cell growth as perturbation to the system. They introduce an adaptive control strategy for the unstable exponential disturbance and are able to hold the ethanol concentration at 0.7 g L^{-1} while the biomass is growing exponentially with a specific growth rate of 0.1 h^{-1}, despite only the overflow metabolite was obtained on-line. Hocalar and Türker [46] are presenting an upscaling of this control approach to a 25 m^3 airlift reactor with on-line ethanol, CO_2, and O_2 measurements. They present good results for

the ethanol control around 0.7 g L^{-1} and high biomass concentration of up to 75 g L^{-1} with a mean specific growth rate of 0.1 h^{-1}.

3.4 Fuzzy logic based control

Fuzzy logic uses linguistic expressions to handle uncertainties. It does not need a mathematical model but rule based process knowledge of an expert operator. In fuzzy control the control action is executed by a predefined rule basis, using rather imprecise linguistic expressions. The expansion of a crisp false and true based logic to a vague partial true linguistic concept is required, because operators are more familiar with it. In fuzzy logic process variables like pH and temperature whose values can be **very high**, **low** or **middle** are formulated in expressions. Therefore fuzzy sets are used to represent these linguistic values. A classical set like A = {x | 5 < x < 7, x $\in \Re$ } contains all real numbers between 5 and 7. An extended version of this classical crisp set is a fuzzy set. A fuzzy set B is defined as a set of ordered pairs B = {(x, $\mu_B(x)$) | x ∈ X, $\mu_B : X \rightarrow [0,1]$ }. Where X contains all elements of measurement values which can occur, $\mu_B(x)$ is the membership function of x in B that maps each element of X to a membership value. An element belongs to a set which is expressed by the membership function to a certain degree that can be a value between 0 and 1 (e.g. the temperature in the reactor is high to a degree of 0.7). The membership function can be of any shape. Triangual, gaussian or sigmoidal functions are often used. To demonstrate the operation of a fuzzy controller a simplified example is presented in Figure 3.4.1 with just two rules:

Rule 1: **If** substrate is *low* OR DO is *high* **then** feeding rate is *high*.
Rule 2: **If** substrate is *high* AND DO is *low* **then** feeding rate is *low*.

The control action is calculated in three steps: 1. Fuzzification, 2. Inference and 3. Defuzzification. In the fuzzification step the membership function is used to calculate the memberschip value of the measurements for the corresponding linguistic term. In the inference step the fuzzy operators (here OR and AND) are applied, which is equal to the maximum and mimumum determination of the membership values of a rule respectively. For each rule the so obtained value is used as upper limit value for the conclusion (then-part) of the rule. During the defuzzification the the output fuzzy sets of all rules are aggregated to one output fuzzy set as shown in Figure 3.4.1. The centroid of the output fuzzy set is calculated as value for the actuating variable of the controller.

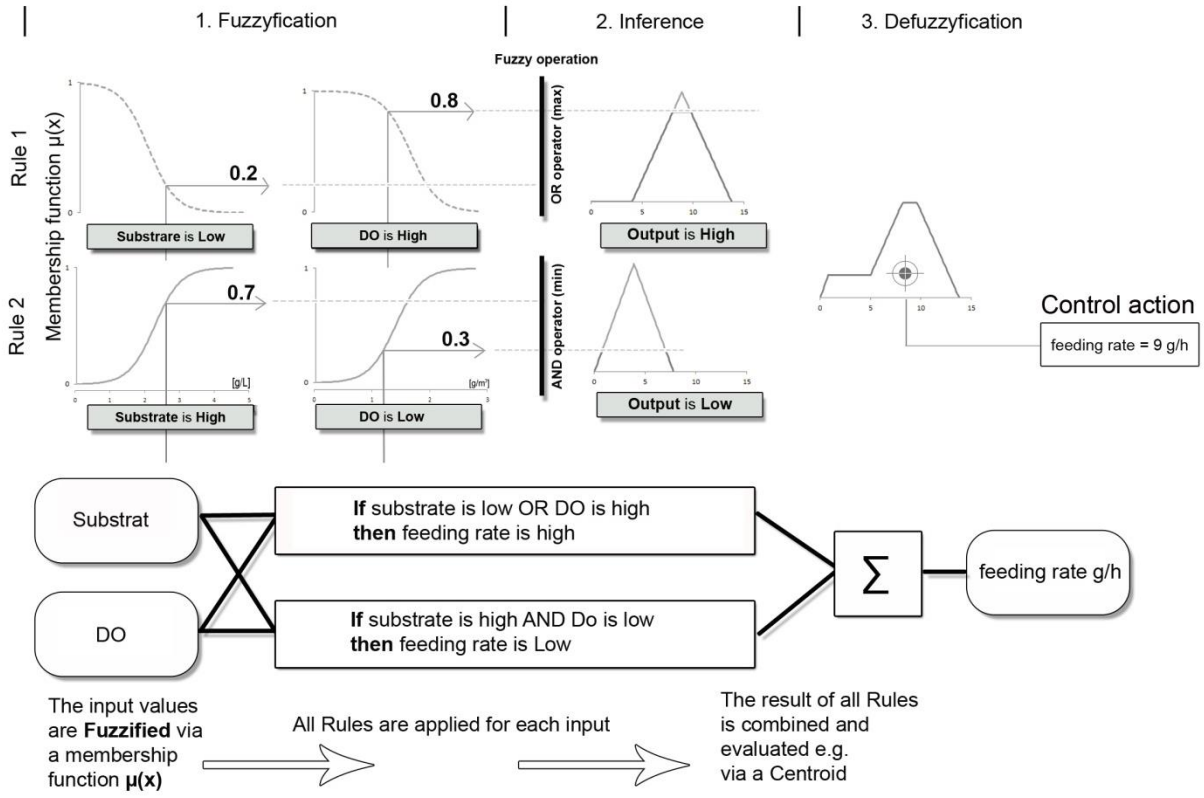

Figure 3.4.1: Basic fuzzy logic scheme for 2 input values, two rules and one output value

A fuzzy controller using 9 rules was implemented by Ruano et al. [47] for a biological nitrification process in a pilot plant with waste water from a full scale plant. Instead of using an expensive nitrogen sensor they employed several pH, ORP (oxidation-reduction potential) and DO sensors. Their fuzzy controller comprises two independent controllers: the nitrification as well as the denitrification process controller. The first one works as a supervisory control of the aeration control system, the second modifies the internal recycle flow rate from the aerobic to the anoxic reactor. The authors demonstrated that using the low-cost sensors in combination with their fuzzy controller leads to a minimized energy consumption of the process.

For the temperature control of a batch reactor Causa et al. [48] compared different versions of a hybrid fuzzy predictive controller. Two on/off input valves and a discrete-position mixing valve were used as controlled variables. The authors concluded that the hybrid fuzzy predictive control in combination with an optimization algorithm based on a genetic algorithm gives similar performance to that of typical hybrid predictive control strategy but a significant saving with respect to the computation time. Compared to a non-linear optimization algorithm [49-51] the genetic algorithms make a time saving of approximately 25 %.

A nonlinear fuzzy controller is presented by Cosenza and Galluzzo [52] for the control of pH and temperature during a penicillin production process. In their application the authors used the so

called type-2 fuzzy set, where uncertainty in the membership function is also implemented. If no uncertainty is present, the membership function is as described above, which is called type 1. In simulations the performance of the type-2 fuzzy controller is compared with an ordinary (type-1) fuzzy controller as well as a PID controller. It was concluded by the authors that due to the nonlinearities and uncertainty of the process the PID controller cannot be compared with the fuzzy controller equitable. The best results were obtained with the type-2 fuzzy controller. When increasing the measurement noise level, the difference between the type-1 and type-2 becomes more clear and evident.

A special controller based on fuzzy logic has been developed by Takagi and Sugeno [53].The difference to the above mentioned fuzzy logic systems is that in the conclusion part a function is defined with the input values as arguments. The conclusion of the whole rule system is the sum of the function values weighted by the corresponding membership functions. Belchior et al. [54] have implemented an adaptive Takagi-Sugeno (TS) fuzzy control algorithm for DO of a activated sludge wastewater treatment process, where the parameter of the conclusion are adapted on-line. The controller has been constructed by using the Lyapunov synthesis approach with a parameter projection algorithm. Parallel to the adaptive control algorithm the authors implemented a supervisory fuzzy control with a smooth switching scheme between supervisory and nonsupervisory modes. In simulations they could demonstrate that the error obtained by the fuzzy controller was less than 2 %, whereas a PI controller produced peaks greater than 10 %

3.5 Artificial neural network based control

Artificial neural networks copy the functionality as well as the structure of biological neural networks by using a mathematical model. In such networks a possible very complex input vector (e.g. visual and/or acoustical signal) can be transferred via various neurons to condense information. Figure 3.5.1 presents a basic artificial neural network (ANN) with four inputs in the input layer, five neurons in the hidden layer and two outputs in the output layer. The structure of an ANN can vary in the number of layers, the connections of the layers and the number of neurons in each layer depending on the complexity the network is supposed to map. Even more outputs than available inputs can be generated. To determine if an artificial neuron “transmits” a signal, all its weighted input values are employed as argument of a transfer function, which can be e.g. sigmoidal functions for smooth transitions or step functions for on/off behavior.

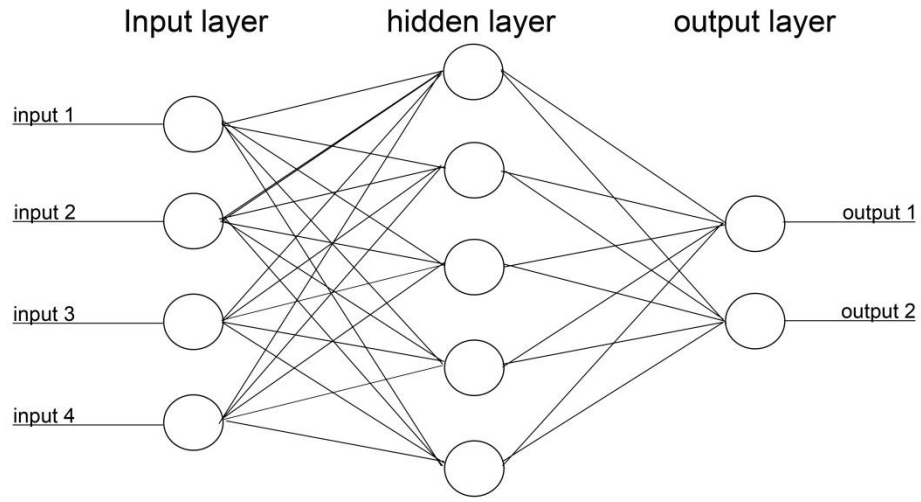

Figure 3.5.1: basic artificial neural network with four inputs in the input layer, five neurons in the hidden layer and one output in the output layer

Corresponding to a biological neural network, an artificial neural network needs to be trained for pattern recognition or decision making. During training the parameters, here called weighting factors, are calculated by an optimization algorithm. The weighting factors are used to weight each input of a neuron. The sum of the weighted inputs is used as argument of the activation function to calculate the output of the neuron. A vast amount of different training data is necessary to build the training sets for a certain problem. A higher variety in the training data leads thereby to better prediction performance of unknown scenarios and prevents that the training data is only memorized.

Karakuzo et al. [55] present an ANN soft-sensor with fuzzy controller for fed–batch fermentations of baker's yeast. The performance of the controller was compared to a controller using a theoretical model-based estimation of the specific growth rate. As input to the network the exhaust gas O_2 and CO_2 concentration, the feeding rate as well as the temperature and pH are used (5 input neurons). The neural network consists of six neurons in the hidden layer and one output neuron to estimate the specific growth rate. For globally robust training data of their ANN, cultivation data sets under a lot of different process conditions were necessary: The authors generated a training data set containing 360 patters and an evaluation data set with the same number of patterns from cultivation data. The results of the model predictive controller they used for comparison gave satisfactory estimation for the specific growth rate, however only under fixed inoculum sizes. The potential of their ANN becomes obvious during the change of inoculum sizes. The ANN continues to generate reliable estimations for the specific growth rate. They also applied a fuzzy logic controller for air flow and feeding control based on the ANN soft-sensor specific growth rate estimation. They performed simulation studies with this controller setup leading to acceptable results for large scale applications.

Gadkar et al. [56] are presenting an on-line adapting neural network as a soft-sensor that estimates the substrate, ethanol and biomass concentration based on dissolved oxygen measurements (1 input neuron, 3 output neurons) during a *S. cerevisiae* fermentation. Their neural network got three hidden layers with ten, eight and four neurons respectively. They discuss the performance with and without an on-line adaption of the weights in the layers of the ANN. Based on the estimation and a mass balance equation the feed rate was calculated by the controller to maintain the glucose concentration at the desired set-point. During controlled substrate fermentations with concentrations between 0.8 g L^{-1} – 1.0 g L^{-1} and a specific growth rate around 0.2 h^{-1} the functional efficiency of the control algorithm is demonstrated. The calculation time for the weight adaption is at 1 – 2 s, allowing an on-line implementation. They admit the need of a priori off-line data, mirroring different cultivation behaviors for training purposes, although in industrial plants such information is usually available. Furthermore, they carried out simulation studies with more than one measured variable and concluded that more than one measured variable will significantly increase the precision of the control. Especially the on-line adaption of the weighting factors of the ANN seems promising, leading to a broader range of its applications even outside the training domain.

3.6 Model predictive control

In the model predictive control (MPC) strategy a dynamic model of a process is applied, to simulate the future evolution of the process depending on possible simulated values of the controlled variable. Typically the future evolution will only be calculated up to a predefined prediction horizon. Using an optimization algorithm the best value of the controlled variable is calculated using a cost function. Due to the fact that a differential equation system must be solved on-line, MPC is computationally demanding. Therefor for MPC a state estimator as well as a controller is required.

The better understanding of penicillin formation mechanisms, morphological features and the role of mycelia for the synthesis led Ashoori et al. [57] to implement a detailed unstructured model of penicillin production in a fed-batch fermenter. This model is used to implement a non-linear MPC (NMPC) for the control of the feed rate to increase the penicillin formation. As controller input they are applying the on-line measurements of pH and temperature. They propose the performance of a novel cost function applying the inverse of the product rather than the common quadratic regulation. This is implemented to avoid ordinary differential equation solver problems where it is not possible to guarantee the efficiency of set-point tracking. They are comparing the control performance to a regular auto-tuned PID controller and identify the NMPC as superior with higher process yields. The NMPC is controlling the acid as well as the base flow and the cooling water

system. Due to the more sophisticated model the control reaches better performance than a previous work by Birol et al. [58]. To face the computational cost of this more detailed model they are proposing the application of a locally linear model tree (LoLiMoT) in order to simplify the original non-linear model, which is described in the next section.

Certainly due to the high computational power that needs to be provided for a MPC many of the NMPC approaches are still only simulation proven and not yet applied to real processes. Santos et al. [59] are working on simulated *E. coli* NMPC controlled cultivations. They assume the measurement of the substrate concentration and keep the specific growth rate at maximum oxidative capacity as well as inhibiting the product formation. They applied a special NMPC scheme named min-max based robustness consideration. Another new NMPC method as well as a comparative performance assessment is applied by Kawohl et al. [10]. They are comparing the performance of NMPC and NMPC – EKF for input signal prediction to a method called on-line trajectory planning (OT). OT is basically an NMPC in which the estimation horizon is extended to the end of the cultivation. If the system is strongly disturbed, this method has certain advantages for the estimation in order to get back to optimal productivity, however at the cost of computational power. The experiments were carried out through Monte Carlo simulations, simulating experiments through disturbance scenarios. The aim of the experiments was to maintain the optimal productivity of the product penicillin. The authors are showing the potential of this closed loop control by improving the mean productivity by 25 % for the MPC and 28 % for the OT method compared to open loop control, where these methods especially increase the minimum productivity due to disturbances.

3.6.1 ANN Fuzzy Hybrid based estimation for NMPC control

A possibility to decrease the complexity of nonlinear models in control algorithms like MPC is given by locally linear models, which are applied in a hybrid structure combining neuronal network and fuzzy logic abilities. The basic structure is displayed in Figure 3.6.2. Each neuron in the hidden layer consists of a membership function and a local linear model (LLM). The arguments of the membership function are the input value x_i. The function value itself indicates the validity of the corresponding LLM, which is in fact a multi linear regression model. The estimate of this model type is the sum of the LLM output weighted by the normalized membership function.

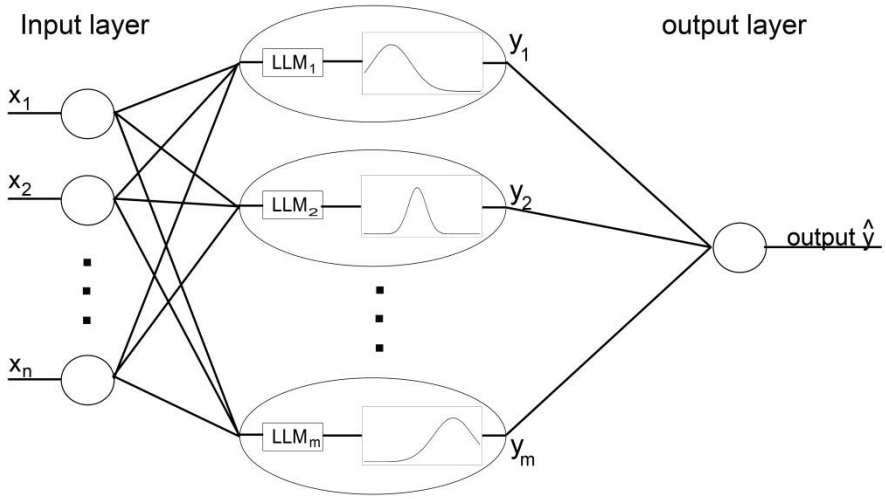

Figure 3.6.1: Basic structure of a Fuzzy-ANN local linear model

The algorithm was successfully applied by Ashoori et al [57] to generate a Neuro–Fuzzy model to replace equations in a mass balance model for penicillin formation. The authors assessed the resulting computational costs as very acceptable for a real time process. They show results which are comparable to results generated by the whole model. Although the method is rarely applied for biotechnological applications, it gives opportunities to overcome frequently mentioned computational limits.

Simulation studies for the optimal model training, parameter identification and comparisons between the closed loop performances are presented by Xu et al. [60-62]. Among others they employed the LOLIMOT algorithm to achieve optimal parameters for the membership function as well as for the LLM. The LOLIMOT algorithm is an incremental tree-based learning algorithm. A detailed description can be found by Nelles [63]. The algorithm adds consecutive locally linear model neurons and thereby optimizes the error of calibration. Obviously a high number of neurons will describe a trajectory best, but will possibly not decrease the computational power that is needed.

3.6.2 ANN based estimation for NMPC

Meleiro et al. [64] presented results of a MPC strategy of a fuel-ethanol fermentation process using simulations. A neural network has been applied as internal model for the controller. The authors used an optimization algorithm to determine a neural network structure as well as the shape of their activation functions guiding to parsimonious network architecture. The inputs were the feed flow rate, cells recycle rate and flash recycle rate; the output were the biomass, substrate and product concentration. The authors presented results demonstrating successfully the control of the biomass,

substrate and ethanol concentration with varying set-points between 37 and 32 gL^{-1}, 10 and 3 gL^{-1} and 45 and 40 gL^{-1}, respectively.

3.7 Probing feeding controller strategy

Velut et al. [65] are presenting a probing feeding strategy for *E. coli* fermentations, operating close to the maximum oxygen transfer rate capacity. The probing feeding strategy principle is to superimpose a short glucose pulse to the glucose feeding flow and evaluate the response in the dissolved oxygen signal. If the dissolved oxygen level decreases the feed rate is increased, due to the determined capacity. If no response can be detected the feeding rate is decreased. The technique is combined with DO control, which is performed by adjusting the stirrer speed and the temperature control to decrease the oxygen demand when the reactor is at its maximum oxygen transfer capacity. They are presenting the performance of the combined controller employing an *E. coli* cultivation. Due to the probing feeding control no acetate was produced. The dissolved oxygen concentration was adjusted to a set point of 30 % over 22 h while decreasing the temperature from 36 °C to 25 °C.

For the probing feeding strategy Velut et al. [66] examined the effect of the reactor scale as well as the influence of different media types. They apply 1.5 min. glucose pulses for lab scale fermenters and longer pulses of 3 min. for large scale fermenters to compensate the slower response. The probing feeding strategy showed good results independent of the medium used. However, the use of a complex medium leads to complications in the interpretation of the pulse response. They determine that the pulsed feeding does not harm the productivity and propose an optimized predetermined feeding trajectory with additional superimposed pulses only for monitoring purposes.

The control strategy is also employed by Xue and Fan [67] for lab and pilot plat (500 L) scale of a recombinant *E. coli* strain producing human-like collagen. For the lab scale experiments they obtained similar results to previous performed optimized studies with 69.1 gL^{-1} dry cell weight and 13.1 gL^{-1} human-like collagen. Compared to previous experiments they observe a reduction of the resulting dry cell weight when applied to the pilot plant. They assume that this results from the different oxygen transfer capacity. However, the resulting collagen with 9.6 gL^{-1} was a satisfying result. They therefore propose a successful application of the probing feeding strategy in a pilot plan scale fermentation process.

3.8 Extremum seeking control

The extremum seeking control is a gradient method to determine on-line unknown parameters throughout the analysis of measurement results as response to a periodical excitation signal called dither. Dochain et al. [68] are presenting a survey on two important classes of extremum seeking to control the perturbation based and the model base method. They investigate the applicability to processes and reaction systems using theoretical models and show the theoretical efficiency of this closed loop control algorithm. Cougnon et al. [69] carried out numerical simulation studies on a fed-batch process model to illustrate their performance for bioprocesses closed loop control. They present an adaptive extremum seeking controller. The controller drives the system to an unknown desired set-point in order to maximize the biomass production. In this contribution the authors assume that the primary carbon source is measurable.

Dewasme et al. [70] are noticing that model based controls are subject to high uncertainty. Therefore they are presenting a model-free extremum seeking strategy on a simulation study of *S. cerevisiae.* They present simulations where the tracking of the critical substrate level (border between fermentative and reparative metabolism) is correctly performed by two different gradient estimation procedures. The input variables for the algorithm are OUR and CPR. The actuating variable is the feeding rate. When parameter uncertainties and noise disturbances occur, they determined a recursive least-squares formulation as simple to implement and better in the resulting set-point tracking.

3.9 Control based on a heuristic procedure

Spectroscopic measurements are providing a wide range of information because of the interaction of electromagnetic radiation with matter. At the same time, this abundance of information is the reason why it is often difficult to interpret. Advanced mathematical tools like partial least squares or principle component analysis are employed to overcome the information overload. Hantelmann et al. [71] are presenting a new method to monitor and control *S. cerevisiae* cultivations by 2D in-situ fluorescence spectroscopy. They introduce a chemometric model that is derived from multivariate data analysis. The glucose feeding rate is thereby controlled predicting the metabolic state directly from the fluorescence intensities. The glucose concentration was held in-between 0.4 and 0.5 gL^{-1} over 11 h, completely avoiding ethanol formations. They point out that the BioView® they used for the cultivation control is suitable for industrial environments.

Schenk et al. [72] are presenting a soft-sensor based on mid-infrared spectroscopy. They introduce a simple and fast method to calibrate the instrument for *Pichia pastoris* fermentations. For this purpose they assume that only the substrate concentration will change significantly during the cultivation and that the absorbance is proportional to the concentration. The control action is performed using a PI – controller. They propose that in some cases like *Pichia pastoris* a multivariate calibration procedure is not necessary and the measurement of one compound of interest is sufficient (in case of *P. pastoris* methanol). The calibration is performed in situ using two points. One spectra at the beginning without carbon source, one with carbon source. They carried out six cultivations in the range of 0.8-15 gL^{-1} to demonstrate the performance of the control system. The standard error of prediction over all cultivations was 0.12 gL^{-1}. They point out that long term baseline instability had an influence on the accuracy, which could be fixed using a linear correction of the signal. Even though the method was designed for the special case of *P. pastoris,* the authors mention a possible application for other microorganisms.

4 Conclusions

In this contribution different approaches of open loop and closed loop control for bioprocess automation are discussed. As a result of the diversity of bioprocess requirements not just one control algorithm can be applied to fulfill all the divers' requirements but different approaches are necessary. During the last 6 years (2006 – 2012) 97 contributions have been published dealing with closed loop control for fermentation processes (ScienceDirect found by "closed loop control" AND fermentation OR cultivation). But only a minority of up to 30 applications was actually applied to real bioprocesses; the majority is based on theoretical applications using simulated processes.

For closed loop control applications in the majority of cases a soft-sensor is combined with a PID controller to determine the feeding rate of substrate or the specific growth rate. This approach can be combined with a forward loop, to reduce the problems generated by the dynamic of the bioprocess. The reason that soft-sensors got this importance for control purposes demonstrate the lack of direct measurements or its big additional expenditure for robust and reliable on-line measurement systems.

Model predictive control has been applied in other application fields successfully and their importance will increase in bioprocess automation as well. However reliable and robust process models are required as well as very powerful computers to provide the computational demand. The lack of theoretical bioprocess models is compensated by hybrid systems combining theoretical

models, fuzzy logic and/or artificial neural networks methodology. These systems are supposed to combine the advantages of each approach to a well performing control strategy.

Some application are made to control fermentations either at their oxidative maximal capacity like the probing feeding approach or the control based on the metabolic state tolerating small amounts of overflow metabolism. Again both approaches demonstrate the lack of necessary direct measurements for important process variables like oxidative capacity or the metabolic state of microorganisms.

Although many authors suggest a possible transfer of their presented control application to other bioprocesses, the algorithms are mostly specialized to a certain organisms or certain cultivation condition as well as to a specific measurement system. The effort to adapt the algorithm and the required measurement system to a specific application is still very high. Therefor in near future the closed loop control of the feeding rate or growth rate will still be a challenge.

However, like Max Planck said: “A new scientific truth does not triumph by convincing its opponents and making them see the light, but rather because its opponents eventually die, and a new generation grows up that is familiar with it.”

Table 3.1 Outline over the employed algorithms, the measured values and the controlled processes presented in this contribution

Measured value	**Actuating variable**	**Controlled process**	**Remarks**	**Employed Algorithm**	**References**
Glucose	Feeding rate	Yeast cultivation		on-off control	Lindgren et. al. [11]
Glucose	Feeding rate	Yeast cultivation / *E. coli*	EKF EKF + ring buffer EKF + Smith Predictor	SISO PID	Arndt and Hitzmann [14] Arndt et al. [15] Kleist et al. [16] Klockow et al. [17] Roever and Slavov [18,19]
	DO, nitrate	Waste water treatment process	Simulation studies	MISO PID	Wahab et al. [20]
OUR, CPR, pH Temperature, DO DO OUR, CPR, DO, V	Feeding rate	*E. coli* *S. cerevisiae* *Fungal fermentation*	Calorimetric model EKF	MISO PID MISO PID cascade	Jenzsch et al. [7] Biener et al. [21] Biener et al. [22] Soons et al. [23] Bodizs et al [24]
OTR, CPR		HCDC	Simulation studies	MIMO PID	Chung et al. [25] Ranjan and Gomes [26]
Ethanol, DO	Feeding rate	*S. cerevisiae* *E.coli*	Industrial fermentation Pilot Plant	RTS controller	Renard et al. [41] [42] Dewasme [43] Cannizzaro et al. [44] Valentinotti et al. [45] Hocalar and Türker [46]
pH, ORP, DO	Recycle flow rate	Nitrification process		Fuzzy logic	Ruano et al. [47]

pH, temperature	Air flow pH, temperature	Penicillin production	Type 2 – fuzzy logic Simulation studies		Cosenza and Galluzzo [52]
Temperature	Temperature		Genetic algorithm	Hybrid Fuzzy logic	Causa et al. [48]
		Waste water treatment process	Simulation studies	TS fuzzy logic	Belchior et al. [54]
O_2, CO_2, feeding rate, temperature, pH	Feeding rate	*S. cerevisiae*	ANN Soft Sensor	Fuzzy logic	Karakuzo et al. [55]
DO	Feeding rate	*S. cerevisiae*	on-line adapting neural network	ANN	Gadkar et al. [56]
pH, temperature	pH, temperature	Penicillin production		NMPC	Ashoori et al. [57]
Substrate	Feeding rate	*E. coli*	Simulation studies NMPC NMPC EKF on-line trajectory planning (OT)	NMPC	Santos et al. [59] Kawohl et al. [10]
Feeding rate, cell recycle rate, flash recycle rate	Biomass, Substrate Ethanol	fuel-ethanol fermentation	ANN model Simulation study	NMPC	Meleiro et al. [64]
DO	Temperature, feeding rate	*E.coli*	 Pilot plant	Probing feeding	Velut et al. [65] Velut et al. [66] Xue and Fan [67]
			Simulation studies	Extremum seeking	Dochain et al. [68]

OUR, CPR	Feeding rate				Cougnon et al. [69] Dewasme et al. [70]
Chemometric model Methanol	Feeding rate Methanol feeding rate	*S. cerevisiae* *Pichia pastoris*	Spectroscopic measurements	heuristic procedures	Hantelmann et al. [71] Schenk et al. [72]

5 References

1. Becker T, Hitzmann B, Muffler K, Pörtner R, Reardon K, Stahl F, Ulber R (2007) Future Aspects of Bioprocess Monitoring. In: Ulber R, Sell D (eds), vol 105. Advances in Biochemical Engineering/Biotechnology. Springer Berlin / Heidelberg, pp 249-293. doi:10.1007/10_2006_036
2. Navrátil M, Norberg A, Lembrén L, Mandenius C-F (2005) On-line multi-analyzer monitoring of biomass, glucose and acetate for growth rate control of a Vibrio cholerae fed-batch cultivation. J Biotechnol 115 (1):67-79. doi:10.1016/j.jbiotec.2004.07.013
3. Warth B, Rajkai G, Mandenius CF (2010) Evaluation of software sensors for on-line estimation of culture conditions in an Escherichia coli cultivation expressing a recombinant protein. J Biotechnol 147 (1):37-45. doi:10.1016/j.jbiotec.2010.02.023
4. Kadlec P, Gabrys B, Strandt S (2009) Data-driven Soft Sensors in the process industry. Computers & Chemical Engineering 33 (4):795-814. doi:10.1016/j.compchemeng.2008.12.012
5. Jain G, Jayaraman G, Kökpinar Ö, Rinas U, Hitzmann B (2011) On-line monitoring of recombinant bacterial cultures using multi-wavelength fluorescence spectroscopy. Biochem Eng J 58–59 (0):133-139. doi:10.1016/j.bej.2011.09.005
6. Jenzsch M, Simutis R, Lübbert A (2006) Generic model control of the specific growth rate in recombinant Escherichia coli cultivations. J Biotechnol 122 (4):483-493
7. Hulhoven X, Wouwer AV, Bogaerts P (2006) Hybrid extended Luenberger-asymptotic observer for bioprocess state estimation. Chem Eng Sci 61 (21):7151-7160. doi:10.1016/j.ces.2006.06.018
8. Kalman RE (1960) A New Approach to Linear Filtering and Prediction Problems. Transactions of the ASME – Journal of Basic Engineering (82 (Series D)):35-45. doi:citeulike-article-id:347166
9. Kawohl M, Heine T, King R (2007) Model based estimation and optimal control of fed-batch fermentation processes for the production of antibiotics. Chemical Engineering and Processing: Process Intensification 46 (11):1223-1241
10. Lidgren L, Lilja O, Krook M, Kriz D (2006) Automatic fermentation control based on a real-time in situ SIRE® biosensor regulated glucose feed. Biosensors and Bioelectronics 21 (10):2010-2013
11. Kriz D, Berggren C, Johansson A, Ansell RJ (1998) SIRE-Technology. Part I. Amperometric Biosensor Based on Flow Injection of the Recognition Element and Differential Measurements. Instrum Sci Technolog 26 (1):45-57. doi:10.1080/10739149808002089
12. Gnoth S, Jenzsch M, Simutis R, Lübbert A (2007) Process Analytical Technology (PAT): Batch-to-batch reproducibility of fermentation processes by robust process operational design and control. J Biotechnol 132 (2):180-186
13. Arndt M, Hitzmann B (2004) Kalman Filter Based Glucose Control at Small Set Points during Fed-Batch Cultivation of Saccharomyces cerevisiae. Biotechnol Prog 20 (1):377-383. doi:10.1021/bp034156p
14. Arndt M, Kleist S, Miksch G, Friehs K, Flaschel E, Trierweiler J, Hitzmann B (2005) A feedforward feedback substrate controller based on a Kalman filter for a fed-batch cultivation of Escherichia coli producing phytase. Computers & Chemical Engineering 29 (5):1113-1120
15. Kleist S, Miksch G, Hitzmann B, Arndt M, Friehs K, Flaschel E (2003) Optimization of the extracellular production of a bacterial phytase with<SMALL> Escherichia coli</SMALL> by using different fed-batch fermentation strategies. Applied Microbiology and Biotechnology 61 (5):456-462. doi:10.1007/s00253-003-1229-3
16. Klockow C, Hüll D, Hitzmann B (2008) Model based substrate set point control of yeast cultivation processes based on FIA measurements. Anal Chim Acta 623 (1):30-37. doi:10.1016/j.aca.2008.06.011
17. Roeva O, Slavov T, Dimov I, Dimova S, Kolkovska N (2008) Fed-Batch Cultivation Control Based on Genetic Algorithm PID Controller Tuning

Numerical Methods and Applications. In, vol 6046. Lecture Notes in Computer Science. Springer Berlin / Heidelberg, pp 289-296. doi:10.1007/978-3-642-18466-6_34
18. Tsonyo S, Roeva O (2011) Genetic Algorithm Tuning of PID Controllerin Smith Predictor for Glucose Concentration Control. Int J BIO Automation 15 (2):101-114

19. Wahab NA, Katebi R, Balderud J (2009) Multivariable PID control design for activated sludge process with nitrification and denitrification. Biochem Eng J 45 (3):239-248
20. Biener R, Steinkämper A, Hofmann J (2010) Calorimetric control for high cell density cultivation of a recombinant Escherichia coli strain. J Biotechnol 146 (1-2):45-53
21. Biener R, Steinkämper A, Horn T (2012) Calorimetric control of the specific growth rate during fed-batch cultures of Saccharomyces cerevisiae. J Biotechnol (0)
22. Soons ZITA, Voogt JA, van Straten G, van Boxtel AJB (2006) Constant specific growth rate in fed-batch cultivation of Bordetella pertussis using adaptive control. J Biotechnol 125 (2):252-268
23. Bodizs L, Titica M, Faria N, Srinivasan B, Dochain D, Bonvin D (2007) Oxygen control for an industrial pilot-scale fed-batch filamentous fungal fermentation. J Process Control 17 (7):595-606
24. Chung YC, Chien IL, Chang DM (2006) Multiple-model control strategy for a fed-batch high cell-density culture processing. J Process Control 16 (1):9-26
25. Ranjan AP, Gomes J (2009) Simultaneous dissolved oxygen and glucose regulation in fed-batch methionine production using decoupled input output linearizing control. J Process Control 19 (4):664-677
26. Davison E (1976) Multivariable tuning regulators: The feedforward and robust control of a general servomechanism problem. IEEE Transactions on Automatic Control 21 (1):35-47. doi:10.1109/tac.1976.1101126
27. Penttinen J, Koivo HN (1980) Multivariable tuning regulators for unknown systems. Automatica 16 (4):393-398
28. M. MJ (1989) Multivariable Feedback Design. 1st printed 1989 edn. Addison-Wiley,
29. Bastin G, Dochain D (1990) On-line estimation and adaptive control of bioreactors, vol 1. Elsevier, Amsterdam ; New York
30. Roeva O, Slavov T, Dimov I, Dimova S, Kolkovska N (2011) Fed-Batch Cultivation Control Based on Genetic Algorithm PID Controller Tuning

Numerical Methods and Applications. In, vol 6046. Lecture Notes in Computer Science. Springer Berlin / Heidelberg, pp 289-296. doi:10.1007/978-3-642-18466-6_34
31. Roeva O (2008) Improvement of genetic algorithm performance for identification of cultivation process models. Paper presented at the Proceedings of the 9th WSEAS International Conference on Evolutionary Computing, Sofia, Bulgaria,
32. Roeva O (2005) Genetic Algorithms for a Parameter Estimation of a Fermentation Process Model: A Comparison. Bioautomation 3:19-28
33. Perrier M, de Azevedo SF, Ferreira EC, Dochain D (2000) Tuning of observer-based estimators: theory and application to the on-line estimation of kinetic parameters. Control Engineering Practice 8 (4):377-388
34. Mazouni D, Ignatova M, Harmand J (2004) A simple mass balance model for biological sequencing batch reactors used for carbon and nitrogen removal. Automatic Systems for building the infrastructure in developing countries
35. Lyubenova V, Ignatova M, Novak M, Patarinska T (2007) Reaction rates estimators of fed-batch process for poly- b-hydroxybutyrate (PHB) production by mixed culture. Biotechnol BioE 21 (1):113–116
36. Ignatova M, Lyubenova V (2007) Control of class bioprocesses using on-line information of intermediate metabolite production and con-sumption rates. Series E: Food Technology 9
37. Ignatova M, Lyubenova V (2007) Adaptive control of fed-batch process for poly-b hydroxybutyrate production by mixed culture. Acad Sci 60 (5):517–524
38. Kansha Y, Jia L, Chiu MS (2008) Self-tuning PID controllers based on the Lyapunov approach. Chem Eng Sci 63 (10):2732-2740
39. Chang WD, Hwang RC, Hsieh JG (2002) A self-tuning PID control for a class of nonlinear systems based on the Lyapunov approach. J Process Control 12 (2):233-242. doi:10.1016/s0959-1524(01)00041-5

40. Renard F, Wouwer AV, Valentinotti S, Dumur D (2006) A practical robust control scheme for yeast fed-batch cultures – An experimental validation. J Process Control 16 (8):855-864. doi:10.1016/j.jprocont.2006.02.003
41. Renard F, Vande Wouwer A (2008) Robust adaptive control of yeast fed-batch cultures. Computers & Chemical Engineering 32 (6):1238-1248. doi:10.1016/j.compchemeng.2007.05.008
42. Dewasme L, Richelle A, Dehottay P, Georges P, Remy M, Bogaerts P, Vande Wouwer A (2010) Linear robust control of S. cerevisiae fed-batch cultures at different scales. Biochem Eng J 53 (1):26-37. doi:10.1016/j.bej.2009.10.001
43. Cannizzaro C, Valentinotti S, von Stockar U (2004) Control of yeast fed-batch process through regulation of extracellular ethanol concentration. Bioprocess Biosyst Eng 26 (6):377-383. doi:10.1007/s00449-004-0384-y
44. Valentinotti S, Srinivasan B, Holmberg U, Bonvin D, Cannizzaro C, Rhiel M, von Stockar U (2003) Optimal operation of fed-batch fermentations via adaptive control of overflow metabolite. Control Engineering Practice 11 (6):665-674. doi:10.1016/s0967-0661(02)00172-7
45. Hocalar A, Tüker M (2010) Model based control of minimal overflow metabolite in technical scale fed-batch yeast fermentation. Biochem Eng J 51 (1):64-71
46. Ruano MV, Ribes J, Seco A, Ferrer J (2012) An advanced control strategy for biological nutrient removal in continuous systems based on pH and ORP sensors. Chemical Engineering Journal 183 (0):212-221. doi:10.1016/j.cej.2011.12.064
47. Causa J, Karer G, Núnez A, Sáez D, Skrjanc I, Zupancic B (2008) Hybrid fuzzy predictive control based on genetic algorithms for the temperature control of a batch reactor. Computers & Chemical Engineering 32 (12):3254-3263
48. Potocnik B, Music G, Zupancic B Model predictive control systems with discrete inputs. In: Electrotechnical Conference, 2004. MELECON 2004. Proceedings of the 12th IEEE Mediterranean, 12-15 May 2004 2004. pp 383-386 Vol.381. doi:10.1109/melcon.2004.1346886
49. Karer G, Mušič G, Škrjanc I, Zupančič B (2007) Hybrid Fuzzy Modelling for Model Predictive Control. Journal of Intelligent & Robotic Systems 50 (3):297-319. doi:10.1007/s10846-007-9166-5
50. Karer G, Musšič G, Škrjanc I, Zupančič B (2007) Hybrid fuzzy model-based predictive control of temperature in a batch reactor. Computers & Chemical Engineering 31 (12):1552-1564
51. Cosenza B, Galluzzo M (2011) Nonlinear fuzzy control of a fed-batch reactor for penicillin production. Computers & Chemical Engineering 36 (0):273-281
52. Takagi T, Sugeno M (1985) Fuzzy identification of systems and its applications to modeling and control. IEEE Transactions on Systems, Man and Cybernetics 15 (1):116-132
53. Belchior CAC, Araujo RAM, Landeck JAC (2011) Dissolved oxygen control of the activated sludge wastewater treatment process using stable adaptive fuzzy control. Computers & Chemical Engineering 37 (0):152-162
54. Karakuzu C, Türker M, Öztürk S (2006) Modelling, on-line state estimation and fuzzy control of production scale fed-batch baker's yeast fermentation. Control Engineering Practice 14 (8):959-974
55. Gadkar KG, Mehra S, Gomes J (2005) On-line adaptation of neural networks for bioprocess control. Computers & Chemical Engineering 29 (5):1047-1057
56. Ashoori A, Moshiri B, Khaki-Sedigh A, Bakhtiari MR (2009) Optimal control of a nonlinear fed-batch fermentation process using model predictive approach. J Process Control 19 (7):1162-1173
57. Birol G, Ündey C, Cinar A (2002) A modular simulation package for fed-batch fermentation: penicillin production. Computers & Chemical Engineering 26 (11):1553-1565
58. Santos LO, Dewasme L, Coutinho D, Wouwer AV (2011) Nonlinear model predictive control of fed-batch cultures of micro-organisms exhibiting overflow metabolism: Assessment and robustness. Computers & Chemical Engineering 39 (0):143-151
59. Xu Z, Zhao J, Qian J, Zhu Y (2009) Nonlinear MPC using an Identified LPV Model. Ind Eng Chem Res 48 (6):3043-3051. doi:10.1021/ie801057q
60. Gong Z (2009) A multistage system of microbial fed-batch fermentation and its parameter identification. Mathematics and Computers in Simulation 80 (9):1903-1910

61. Lawryńczuk M (2011) Online set-point optimisation cooperating with predictive control of a yeast fermentation process: A neural network approach. Engineering Applications of Artificial Intelligence 24 (6):968-982. doi:10.1016/j.engappai.2011.04.007
62. Nelles O (2001) Nonlinear System Identification. Springer,
63. Meleiro LAC, Von Zuben FJ, Filho RM (2009) Constructive learning neural network applied to identification and control of a fuel-ethanol fermentation process. Engineering Applications of Artificial Intelligence 22 (2):201-215. doi:10.1016/j.engappai.2008.06.001
64. Velut S, de Marco L, Hagander P (2007) Bioreactor control using a probing feeding strategy and mid-ranging control. Control Engineering Practice 15 (2):135-147
65. Velut S, Castan A, Short KA, Axelsson JP, Hagander P, Zditosky BA, Rysenga CW, De Maré L, Haglund J (2007) Influence of bioreactor scale and complex medium on probing control of glucose feeding in cultivations of recombinant strains of Escherichia coli. Biotechnol Bioeng 97 (4):816-824. doi:10.1002/bit.21294
66. Xue WJ, Fan DD (2011) Fed-batch production of human-like collagen with recombinant Escherichia coli using feed-up DO-transient control. Huaxue Gongcheng/Chemical Engineering (China) 39 (10):6-10
67. Dochain D, Perrier M, Guay M (2011) Extremum seeking control and its application to process and reaction systems: A survey. Mathematics and Computers in Simulation 82 (3):369-380. doi:10.1016/j.matcom.2010.10.022
68. Cougnon P, Dochain D, Guay M, Perrier M (2011) On-line optimization of fedbatch bioreactors by adaptive extremum seeking control. J Process Control 21 (10):1526-1532. doi:10.1016/j.jprocont.2011.05.004
69. Dewasme L, Srinivasan B, Perrier M, Vande Wouwer A (2011) Extremum-seeking algorithm design for fed-batch cultures of microorganisms with overflow metabolism. J Process Control 21 (7):1092-1104. doi:10.1016/j.jprocont.2011.05.002
70. Hantelmann K, Kollecker M, Hüll D, Hitzmann B, Scheper T (2006) Two-dimensional fluorescence spectroscopy: A novel approach for controlling fed-batch cultivations. J Biotechnol 121 (3):410-417. doi:10.1016/j.jbiotec.2005.07.016
71. Schenk J, Marison IW, von Stockar U (2007) A simple method to monitor and control methanol feeding of Pichia pastoris fermentations using mid-IR spectroscopy. J Biotechnol 128 (2):344-353. doi:10.1016/j.jbiotec.2006.09.015

Chapter

3

Automated sonic velocity calculation based on ultrasonic resonator measurements for on-line process monitoring

M. Stanke, P. Lindner, S. Holz, B. Hitzmann (2013),

Sensors and Actuators A: Physical, 198: 69-74

Abbreviations and nomenclature

Value	Description	Unit
τ_G	group delay time	$1 \cdot s^{-1}$
φ	phase angle	rad
ω	angular frequency	$rad \cdot s^{-1}$
n	harmonic order	1
f_n	resonance frequency with harmonic order n	Hz
f_L	fundamental frequency of the liquid loaded cavity	Hz
z_L	impedance liquid	$Kg \cdot m^{-2} \cdot s^{-1}$
z_T	impedance transducer	$Kg \cdot m^{-2} \cdot s^{-1}$
f_T	fundamental frequency transducer	Hz
σ	dispersion factor	1
D	resonator length	m
c_L	sonic velocity of the liquid loaded cavity	$m \cdot s^{-1}$
c_L^{Lit}	literature (reference) value of the sonic velocity	$m \cdot s^{-1}$
Δc_L^{Lit}	uncertainty of the reference value	$m \cdot s^{-1}$
Δ_{c_L}	uncertainty of the sonic velocity	$m \cdot s^{-1}$
Δf_L	uncertainty fundamental frequency	Hz
Δ_D	uncertainty resonator length	m

Abstract

Many applications of sonic velocity measurements for material testing are known and widely employed. Yet the technique is rarely employed in biotechnology especially for process monitoring. The ultrasonic resonator technology allows a highly precise measurement of the sonic velocity in small volumes, which makes this technology interesting for process analytics. New techniques give information about various process parameters on-line and in real time. Nowadays special interest is the on-line product analytic. Not only is the product concentration is in focus, but the purity and activity, which are currently rarely accessible on-line. The ultrasonic resonator is an opportunity to close this gap. An evaluation method will be introduced to ensure a maximum in precision and accuracy during the measurement. The best obtained precision of less than 0.3 $mm \cdot s^{-1}$ sonic velocity and an accuracy of 0.027 $m \cdot s^{-1}$, for water at different temperatures, give the possibility to detect slightest changes and recover worthwhile information during the measurements.

Keywords: ultrasonic resonator, sonic velocity evaluation, protein detection, protein folding, on-line process monitoring

1 Introduction

The fermentation industry is a constantly growing sector and especially the development of new products and manufacturing methods are not only growing, but also changing. Real time process monitoring is fundamental for an efficient process control [1](Vojinovic, Cabral et al. 2006). In the past years the classical off-line analytic has been displaced from process accompanying methods to development only methods. Nowadays the aim is to give a robust and reproducible high quality process evaluation on-line and in real time. Different strategies are employed to obtain this for biological or chemical processes. [1](Vojinovic, Cabral et al. 2006). Especially noninvasive methods based on chemometrical data evaluation are growing more and more. New technologies like the recently upcoming Raman spectroscopy and the mid / near infrared spectroscopy as well as the fluorescence spectroscopy can possibly give information about a wide range of process variables such as glucose, ethanol, lactic acid and biomass concentration [2-5](Solle, Geissler et al. 2003; Roychoudhury, Harvey et al. 2006; Kim, Hwang et al. 2008; Shih and E. A. 2009). Many applications for ultrasonic measurements are known and widely employed, especially as distance sensors [6](Henning and Schröder 2011), but only rarely as sonic velocity measurements for process analytics. Krause et al. [7](Krause, Schöck et al. 2011) describe a sonic time of flight measurement system using a pulse-echo method for on-line ethanol and glucose concentration characterization.

No commercially available device is yet capable to detect the folding state of solvated proteins on-line. In particular the pharmaceutical industry is in need of effective techniques not just concerning product concentration but purity and activity. Ultrasonic resonator measurements have already been applied as a suitable process analytical tool for pharmaceutical problems [8](Cavgen, Douglas et al. 2011). Protein purification is also an ubiquitary occurring topic. There are several crucial steps that can compromise the protein folding, which is strictly correlated to activity. That can be for example during the inclusion body processing or the purification via a column. Since the recent breakthrough in the THz absorption spectroscopy [9](Scheller and Koch 2009) a new method at presumably low cost is available for high precision spectroscopy. A research group around Havenith has been working on that technology for some time now [10-12](Heugen, Schwaab et al. 2006; Ebbinghaus, Kim et al. 2007; Kim, Born et al. 2008). The method is highly sensitive and capable to give information about the solvation dynamics of solutions. Born et al. [13](Born, Kim et al. 2009) describe that even a single phenylalanine-to-tryptophan substitution leads to a detectable change in the solvation dynamics. However, there are no practical applications yet.

Here an on-line monitoring system based on sonic velocity measurements will be introduced. Eggers gave an approach to calculate the sonic velocity from an ultrasonic resonator [14, 15](Eggers 1967; Eggers 1997). Based on that approach an automated on-line capable evaluation procedure was developed. The sonic velocity is a material constant whose square is inversely proportional to the product of adiabatic compressibility κ_{ad} and the density ρ. Different folding states will lead to different values for compressibility and therefore different sonic velocities. E.g. an unfolded protein is less compressible than a complex folded protein with α-helices, β-sheets and enclosed water molecules. This technology has been found sensitive enough to be a possible technique to detect protein folding and even different folding pathways. Smirnovas et al. [16, 17](Smirnovas, Winter et al. 2005; Smirnovas and Winter 2008) showed that the sonic velocity obtained by the ultrasonic resonator can be correlated to other protein analytic methods and give distinct different measurement results for varying aggregation pathways. A detection system has been realized for an on-line observation of protein related processes which allows access to the parameter folding. Here results for an optimal evaluation of ultrasonic resonator measurements are presented to accomplish a maximum in precision and accuracy.

2 Theory and instrumentation

2.1 Sample preparation and process link

In Figure 1 the experimental setup is presented as well as the actual measurement cavity. The measurement is realized as a reference method. Two volume flows are directed through a dialysis system to even the distinctions between the reference and the sample.

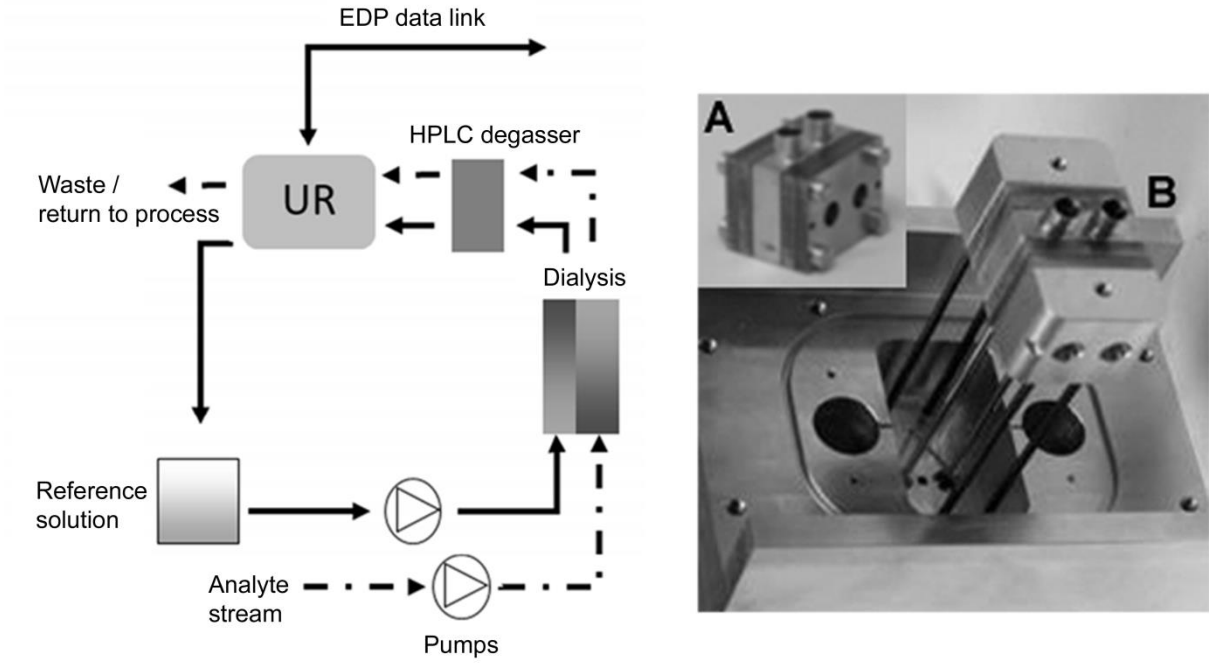

Figure 1 (left) Scheme of the experimental setup. The scattered line is the analyte stream the draw through line is the reference stream. They will be equalized in the dialysis and measured in the UR block. Based on the process the analyte stream can be returned or disposed. (right) (A) Picture of the resonator cavity. (B) Resonator cavity in the copper block slit.

The pore size of the dialysis membrane is selected in a way that proteins cannot pass. A degassing unit is applied to prevent air bubbles from rising into the measurement cell which would disturb the measurement signal significantly. At the point where the volume flow reaches the ultrasonic resonator (UR) the only difference between the two solutions should be the proteins.

2.2 Data acquisition and evaluation

The actual measurement unit contains a titan block with a cavity enclosed by two gold-layered $LiNbO_3$ piezoelectric elements. On one side of the cavity a waveform generator leads the

piezoelectric element to vibrations; on the other side of the cavity a second piezoelectric element's function is to act as a receiver. With assistance of an electrical reference circuit the output signals of the resonator for a certain input frequency are the amplitude, the phase angle φ and the group delay time τ_G:

$$\tau_G = -\frac{d\varphi}{d\omega} \qquad (1)$$

with ω the angular frequency. Due to the complex electro-mechanical coupling between the liquid and the piezoelectric material itself, the system does not behave ideally harmonic, but inharmonic. As a consequence the fundamental frequency which is needed to determine the sonic velocity cannot be measured directly. Therefore an extensive data evaluation is needed. Figure 2 displays a characteristic series of resonant frequencies, which have to be determined precisely. This series of frequencies is used by Equation 2 to calculate the fundamental frequencies [14, 15](Eggers 1967; Eggers 1997).

$$f_n = f_L \cdot \left[n + \frac{2}{\pi} \cdot \operatorname{atan}\left(\frac{z_L}{z_T} \cdot \cot\left(\pi \cdot \frac{f_n}{f_T} \right) \right) \right] \qquad (2)$$

With f_L the fundamental frequency of the liquid-loaded cavity, f_n resonance frequency with harmonic order n (also called normal modes or overtones), f_T fundamental frequency of the transducer, z_L impedance of the liquid, z_T impedance of the transducer. The prediction preciseness was further improved by Kononenko [18](Kononenko 1997). He took the diffraction phenomenon in both the liquid and the piezoelectric transducers into account. With his work the prediction of the inharmonic resonant conditions is more accurate. Therefore Equation 3 is used for the data evaluation which is the model described by Eggers [15](Eggers 1997)

$$f_n = f_L \cdot \left[n + \frac{2}{\pi} \cdot \operatorname{atan}\left(\frac{z_L}{z_T} \cdot \cot\left(\pi \cdot \frac{f_n \cdot \left(\sigma \cdot \frac{(f_n - f_T)}{f_T} \right)}{f_T} \right) \right) \right] \qquad (3)$$

with σ as a dispersion factor introduced by Kononenko [18](Kononenko 1997).

2.3 Estimation of the theoretical error for the absolute sonic velocity determination

For the uncertainty propagation calculation the following equation will be used.

$$\Delta_p(p_1..p_n) = \left[\sum_{i=1}^{n} \left(\frac{\partial F}{\partial p_i} \cdot \Delta p_i \right)^2 \right]^{\frac{1}{2}} \qquad (4)$$

Equation 5 is applied to determine the sonic velocity out of the fundamental frequency f_L of the liquid loaded cavity obtained out of Equation 3.

$$c_L = 2 \cdot D \cdot f_L \qquad (5)$$

After rearrangement of Equation 5 and with a reference value for the sonic velocity c_L^{Lit}, the distance D can be calculated as $D = c_L^{Lit} \cdot 2{f_L}^{-1}$. Using Equation 6 one can calculate the uncertainty to the resonator length caused by the calibration due to a known sonic velocity and its uncertainty Δc_L^{Lit} at temperature T.

$$\Delta_D(T) = \left[\left(\frac{-c_L^{Lit}(T)}{2{f_L}^2} \cdot \Delta f_L\right)^2 + \left(\frac{1}{f_L} \cdot \Delta c_L^{Lit}\right)^2\right]^{\frac{1}{2}} \qquad (6)$$

With known uncertainty of the resonator length one can calculate the uncertainty of the absolute sonic velocity calculation using the variance of the fundamental frequency determination ${\Delta f_L}^2$ and Equation 7.

$$\Delta_{c_L}(T) = [(2f_L \cdot \Delta_D(T))^2 + (2D \cdot \Delta f_L)^2]^{\frac{1}{2}} \qquad (7)$$

2.4 Software and instrumentation

The control and evaluation software was programmed in Visual C# .Net Framework 4.0. The computer system needed to run the software must at least support Windows XP Service Pack 2.

The measurement system is an ultrasonic resonator based on the ultrasonic resonator technology of the company TF-Instruments (Heidelberg, Germany) modified for flow-through operations. These modifications include an inflow and an outflow on opposite sides rather than one opening in the measurement cavity.

Temperature constancy better than 10^{-3} K between 5 °C and 85 °C of the Peltier thermostat is specified by the manufacturer, which has been verified (data not shown). The ultrasonic resonator is equipped with a control unit which provides a basic control of the measurements. The maximal measurement range of the device is from 6.6 MHz to 11 MHz deviating between resonators, due to fabrication variances of the piezo-ceramics. Two data acquisition modes are available: Measurements with predetermined frequency steps and measurements employing a Phase Loop Lock (PLL). The Frequency mode provides two operating modes: An *extended range scan,* measuring the whole range with a step size of 15 kHz and an *operating range scan* providing the frequency range from 7.1 – 8.9 MHz in 6.5 kHz steps.

The PLL mode provides a control system that adjusts the oscillator frequency to keep to phases matched. The system can be combined with the *operating range scan*. On a phase shift between two resonant frequencies the PLL pulls the oscillator frequency to the next overtone. This mode gives crude information (variance of ~625 Hz) for the actual resonant frequency maximum. The last mode

is a *fine scan mode* applying also the PLL. The maximal range of the *fine scan mode* is ~400 kHz around a given frequency (typically obtained from the *PLL operating range scan*). The step size deviates between 10 Hz and 4 kHz for the whole range and around the resonance peak maximum between 10 – 40 Hz. This leads to a high resolution resonance peak which is used for further evaluations. Because of the fact that the frequency steps are automatically chosen, the measurement points are rarely equidistant and uneven gaps occur.

The device is designed as an on-line process monitor for aqueous solutions. Therefore the evaluation procedure will be presented using 19 measurements of deionized water between 20-30 °C, each with ten resonance frequencies between 7.5 MHz and 8.5 MHz. The well described dependency of the sonic velocity to the temperature down to 0.02 $m \cdot s^{-1}$ [19-21](Bilaniuk and Wong 1993; Erratum:, Bilaniuk et al. 1996; Marczak 1997) serves as a reference to calculate the accuracy of the evaluation. Values in between were interpolated using a polynomial of 3rd degree. To exclude disturbances the pump rate was kept very low at 0.01 $ml \cdot min^{-1}$.

3 Results and discussion

The calculation of the sonic velocity is performed in two steps. First step is the determination of the resonant frequencies. Second step is the calculation of the sonic velocity from these resonant frequencies. The resonance frequency determination can be achieved using the amplitude maxima as well as the position of the group delay time maxima. Therefore a comparative evaluation is presented.

3.1 Determination of resonance frequencies

Decisive for the precision is the preferably exact determination of the resonant frequency, which can be calculated from either the group delay time maximum or the amplitude maximum. In order to determine the resonant frequency the approach is to fit an analytical function to the resonant peak and calculate the position of the maximum of that function. An approach for an analytical function is the Lorentz profile which describes the natural line width. The amplitude is considerably affected by two effects. The first effect is the base line elevation of the resonant peaks with increasing frequency which can be seen in Figure 2.

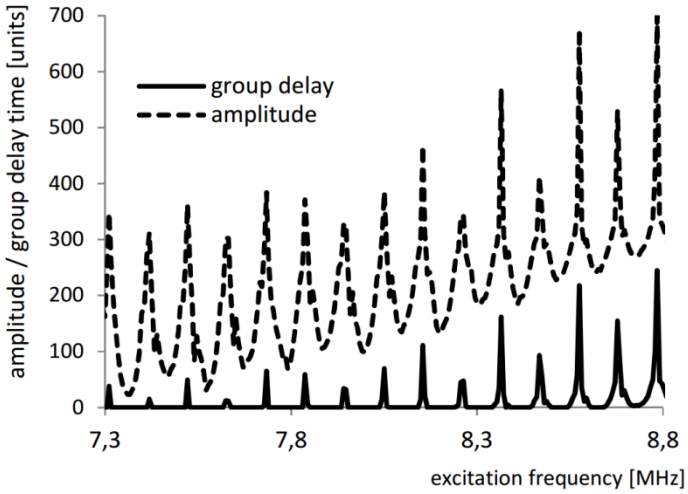

Figure 2 Measurement between 7.3 MHz and 8,8 MHz excitation frequency. The step size of excitation is ~6.5 kHz. Displayed data for group delay time and amplitude values in units. Each peak represents a resonant peak. The strong differing heights are due to the resolution not always hitting the tip of the peaks.

This is an effect caused by the resonant peak of the piezo-ceramic which is also a system capable to oscillate. This effect leads to an angular dislocation of the peaks. The amplitude information is more effected by this elevation than the group delay time. Secondly and in agreement with Kaatze et al. [22](Kaatze, Lautscham et al. 2000) it can be confirmed that the amplitude peaks are showing distinct satellite peaks on both flanks, which can be seen in Figure 3a. The two satellites cannot be measured completely because of the PLL usage, ensuring the measurement of the actual resonant peak. For comparison Figure 3b shows the group delay time at the same excitation frequency. These satellites influence the fit of the Lorentz profile and therefore the determination of the maxima. Both facts lead to the assumption, that a fit of the whole peak is not the method of choice. Experiments have shown that a fit to the whole peak leads to a less precise evaluation of the peak maximum especially for the amplitude. Figure 4 shows this relation. The maximum evaluation was compared to a manually performed interpolation of the data to find the maximum of 30 measured resonant peaks. Using only the tip (10 %) of the amplitude and group delay peaks leads to the most precise resonant peak evaluation, although there is only a slight improvement in the group delay time evaluation. Slightly better results can also be obtained by using a polynomial of fourth degree although the Lorenz profile is advantageous for automatic processing due to the default shape and therefore less failure-prone.

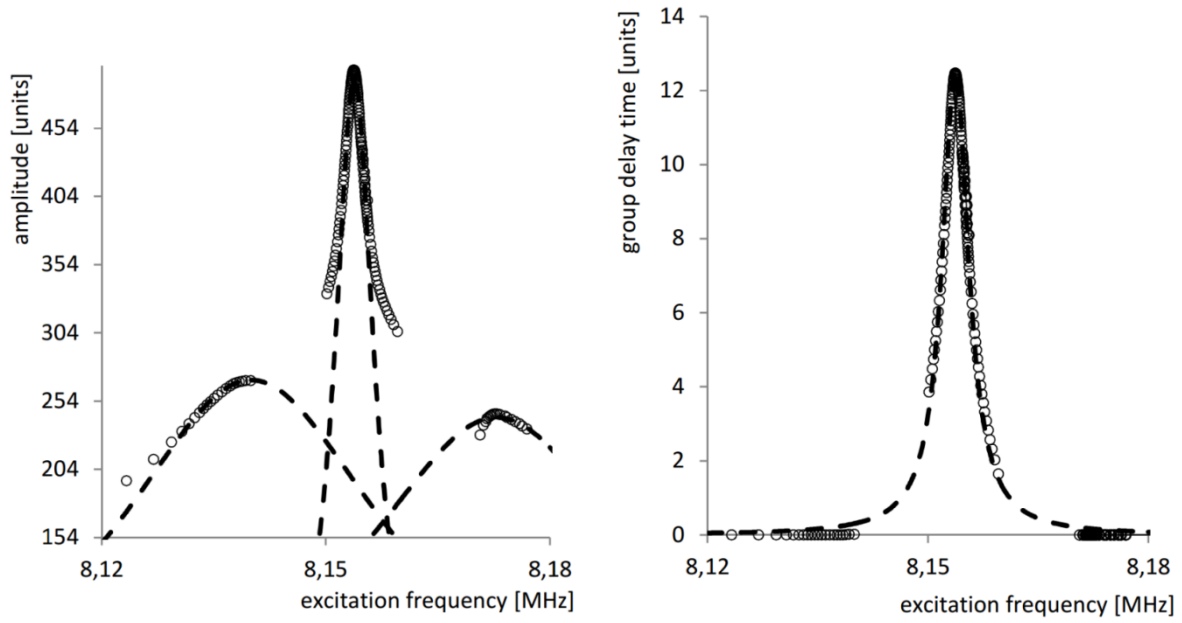

Figure 3a High resolution scan of the amplitude resonant peak with flanking satellites. Scattered lines are fitted Lorentz profiles. The amplitude peak is superposed signal of more than one resonant peak.

Figure 3b High resolution scan of the group delay time resonant peak at the same excitation frequency as the amplitude peak in Figure 3a.The Scattered line is a fitted Lorentz profile.

Another benefit of not using the whole peak is the obvious reduction of data points, speeding up the measurement. Keeping in mind that the evaluation needs to be designed for a flow through system, a reduced measurement time is of interest.

3.2 Calculation of the sonic velocity and uncertainty propagation

From the series of resonant frequencies the impedance ratio z_L/z_T as well as the fundamental frequency of the liquid-loaded cavity f_L can be numerically solved using Equation 8. In Table 1 the determined resonant maxima between the harmonic order n=71..79 of deionized water at 21 °C and 27 °C are given. Applying a constrained nonlinear multivariable optimization algorithm (e.g. Matlab® fmincon) can solve the problem described in Equation 8

$$f\left(f_L, \frac{z_L}{z_T}\right) = \sum_{n=71}^{79}\left(f_L \cdot \left[n + \frac{2}{\pi} \cdot \operatorname{atan}\left(\frac{z_L}{z_T} \cdot \cot\left(\pi \cdot \frac{f_n \cdot \left(\sigma \cdot \frac{(f_n - f_T)}{f_T}\right)}{f_T}\right)\right)\right] - f_n\right)^2 = min \qquad (8)$$

using z_L/z_T and f_L as variables for the algorithm and the parameter f_T = 9313367.457 Hz and for σ = 1.2. This will lead to results described at the bottom of Table 1.

With the calculated impedance ratio, a fundamental frequency can be calculated from each resonance frequency. The advantage is that further measurements only need to be applied to one resonant frequency. The change in sonic velocity will be described due to the differing position of that particular peak, which can be determined precisely, as discussed above. Though, Equation 3 is only correcting the inharmonic behavior of the resonator and is as well subject to the error that is caused by the resonator geometry displacement. That was also proposed by Padilla et al. [23](Padilla, Gindre et al. 2001) for this system, who gave an attempt for a new mathematical model to solve this problem. To display the error that occurs during the measurement a brief error analysis will be given.

For the presented data sets a standard deviation of Δc_{LL}=0.02 m·s^{-1} is calculated for all literature values of 20 °C - 30 °C. Applying Equation 6 is leading to a mean standard deviation for the resonator distance D (Δ_D) of 1.11·10^{-7} m.

The mean standard deviation for the absolute sonic velocity calculation over all test sets is 0.45 m·s^{-1}. In the literature [15](Eggers 1997) is suggested to increase the accuracy by taking a “well-chosen” resonant peak for each velocity calculation. The criteria to choose though are not given.

In this contribution a polynomial correction function is used for the fundamental frequencies which lead to a much less variant data. The corrected fundamental frequencies $f_{Lc}(\omega)$ can be obtained as

$$\boldsymbol{f_{Lc}(\omega) = \left(f_L(\omega) - p(\omega)\right) + \frac{1}{n}\sum_1^n f_L(\omega).} \qquad (9)$$

with $\mathbf{f_L(\omega)}$ fundamental frequency of the liquid loaded cavity at frequency $\boldsymbol{\omega}$ and $\boldsymbol{p(\omega)}$ the function value of the polynomial of 3rd degree at the frequency $\boldsymbol{\omega}$. An uncorrected and corresponding corrected data set can be seen in Table 2 and Table 3 respectively. Although the actual fundamental frequency is not calculated in this step, all resonant frequencies will lead to the same sonic velocity within a standard deviation of 0.011 m·s^{-1} and therefore, by using this procedure, a high reproducible value for the sonic velocity is obtained. The mean standard deviation for the absolute sonic velocity, applying Equation 7 again, is 0.027 m·s^{-1} using the corrected values for the fundamental frequency of the liquid loaded cavity.

The cell length of the cavity is calibrated with an analyte of known sonic velocity (e.g. water at a certain temperature). Therefore a defect that probably emerges due to the baseline correction is displaced to the cavity cell length. There is an error to the actual fundamental frequency, but measurements of the sonic velocity will be recovered correctly. Since the aim is the reproducible

determination of the sonic velocity, an uncertainty for the cell length and fundamental frequency seems to be tolerable. The best recovery rate was 9 mm·s^{-1}.

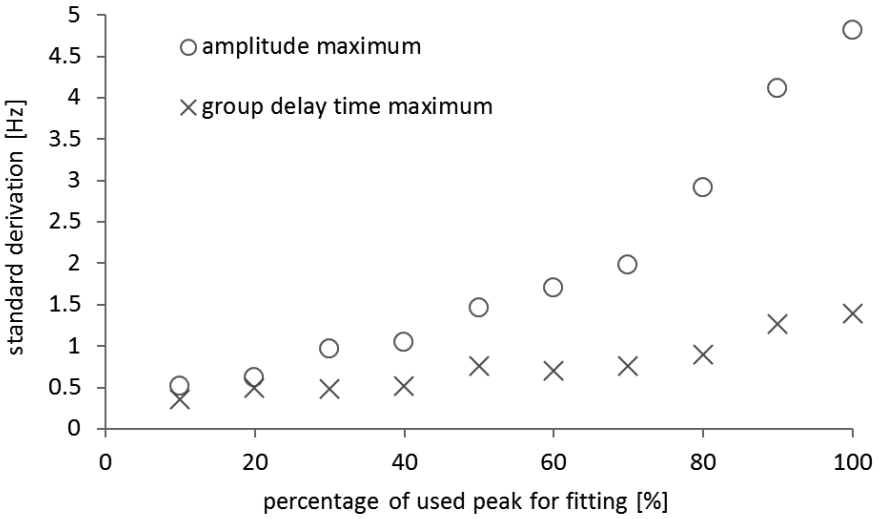

Figure 4 Standard deviation of peak maximum determination dependent to the percentage of used peak information for fitting. 100% is the full peak. 10% (of the peak height) only the tip. Data obtained from 30 resonance peaks between 7.4 MHz and 8.7 MHz. The peak maximum evaluation was obtained using a Lorentz profile and a Simplex algorithm.

Comparable, recently published methods like precise time of flight measurements e.g. by Rodrígues López et al. [24](Rodríguez-López, Segura et al. 2012) showing precisions of 30 mm·s^{-1} sonic velocity. A comparable resonator method (Sonas Technologies) as described by Pablo and Buckin [25](Resa and Buckin 2011) is showing similar reproducibility of 0.3 mm·s^{-1} and a comparable, but lower accuracy of 0.5 m·s^{-1}. A totally new approach using echo signals from scattering particles as described by Lenz et al. [26](Lenz, Bock et al. 2011) shows uncertainties of up to 50 m·s $^{-1}$.

4 Conclusions

An evaluation method for a precise on-line capable sonic velocity determination from ultrasonic resonators has been presented. It has been shown that significant differences in the precision of the evaluation are reached according to the resonator signal that is used for the sonic velocity determination. The best results could be obtained using only the tip of the group delay time resonant peak; here the standard deviation for the repetitive sonic velocity determination (precision) was $3 \cdot 10^{-4}$ m·s^{-1}. Secondly and more important for the automation capability a new evaluation method

was presented for the determination of the sonic velocity. The accuracy of the device could be improved using a simple polynomial correction to 0.027 $m \cdot s^{-1}$.

5 Acknowledgements

The authors are grateful to the BMBF. Without their support the project and the research could not have been done. We would also like to thank all members of the project “Proteinmonitor” for the collaboration representative: Dr. W. Künnecke (*TRACE Analytics GmbH*), Prof. Dr. T. Scheper *(Universität Hannover),* J. Peters (*TF Instruments GmbH*), Prof. R. Winter (*Technische Universität Dortmund),* Dr. D. Riechers *(Sartorius Stedim Biotech)*.

[1] V. Vojinovic, J.M.S. Cabral, L.P. Fonseca, Real-time bioprocess monitoring, Sens Actuators B: Chem2006, pp. 1083-91.

[2] P. Roychoudhury, L.M. Harvey, B. McNeil, The potential of mid infrared spectroscopy (MIRS), Anal Chim Acta2006, pp. 159-66.

[3] J. Kim, J. Hwang, H. Chung, Comparison of near-infrared and Raman spectroscopy for on-line monitoring of etchant solutions directly through a teflon tube, Anal Chim Acta2008, pp. 119-27.

[4] C. Shih, S. E. A., Determination of glucose and ethanol after enzymatic hydrolysis and fermentation of biomass using Raman spectroscopy, Anal Chim Acta2009, pp. 200-6.

[5] D. Solle, D. Geissler, E. Stärk, T. Scheper, B. Hitzmann, Chemometric Modeling based on 2D Fluorescence Spectra without a Calibration Measurement, Bioinformatics2003, pp. 173-7.

[6] B. Henning, A. Schröder, Ultrasonic distance sensors - An overview and trends, J Elec Meas Inst2011, pp. 577-81.

[7] D. Krause, T. Schöck, M.A. Hussein, T. Becker, Ultrasonic characterization of aqueous solutions with varying sugar and ethanol content using multivariate regression methods, J Chemomometrics2011, pp. 216-32.

[8] M. Cavgen, R. Douglas, G. Akkermans, M. Kuentz, Study of an ultrasound-based process analytical tool for homogenization of nanoparticulate pharmaceutical vehicles, J Pharm Sci2011, pp. 3374-85.

[9] M. Scheller, M. Koch, Terahertz quasi time domain spectroscopy, Opt Express2009, pp. 17723-33.

[10] S. Ebbinghaus, S.J. Kim, M. Heyden, X. Yu, U. Heugen, M. Gruebele, et al., An extended dynamical hydration shell, Proc Natl Acad Sci U S A2007, pp. 20749-52.

[11] S.J. Kim, B. Born, M. Havenith, G. Martin, Real-time detection of protein–water dynamics upon protein, Angew Chem2008, pp. 6486-9.

[12] U. Heugen, G. Schwaab, E. Bründermann, H. M., X. Yu, D.M. Leitner, et al., Solute-induced retardation of water dynamics probed, Proc Natl Acad Sci U S A2006, pp. 12301-6.

[13] B. Born, S.J. Kim, S. Ebbinghaus, M. Gruebele, M. Havenith, The terahertz dance of water with the proteins, Faraday Discuss2009, pp. 161-73.

[14] F. Eggers, Eine Resonatormethode zur Bestimmung von Schall-Geschwindigkeit und Dämpfung an geringen Flüssigkeitsmenegen, Acoustica1967, pp. 323-9.

[15] F. Eggers, Model calculation for ultrasonic plate-liquid-plate resonators: peak frequency shift by liquid density and velocity variations, Mess Sci Technol1997, pp. 643-7.

[16] V. Smirnovas, R. Winter, Revealing different aggregation pathways of amyloidogenic proteins by, Biophys J2008, pp. 3241–6.

[17] V. Smirnovas, R. Winter, T. Funck, W. Dzwolak, Thermodynamic properties underlying the r-Helix-to-â-sheet transition, aggregation, and amyloidogenesis of polylysine as probed by calorimetry, densimetry, and ultrasound, J Phys Chem2005, pp. 19043-5.

[18] V.S. Kononenko, Precise measurments of elastic wave velocity and dispersion in liquids by an ultrasonic resonator with plane piezoelectric plates, Acoust Phys1997, pp. 354-6.

[19] N. Bilaniuk, G. Wong, Speed of sound in pure water as a function of temperature, J Acoust Soc Am1993, pp. 1609-12.

[20] Erratum:, N. Bilaniuk, G.S.K. Wong, Erratum: Speed of sound in pure water as a function of temperature, J Acoust Soc Am1996, pp. 3257-.

[21] W. Marczak, Water as a standard in the measurments of speed of sound in liquids, JAcoust Soc Am1997, pp. 2776-9.

[22] U. Kaatze, K. Lautscham, F. Wente, S. W., High resolution and snall volume automatic ultrasonic velocimeter for liquids, Meas Sci Technol2000, pp. 1432-9.

[23] F. Padilla, M.l. Gindre, J. Le Huérou, Model and measurements of the electrical imput impedance of a plate-liquid-plate acoustic resonator, IEEE Trans Ultrason, Ferroelectr Freq Control2001, pp. 838-43.

[24] J. Rodríguez-López, E.L. Segura, F. Montero de Espinosa Freijo, Ultrasonic velocity and amplitude characterization of magnetorheological fluids under magnetic fields, JMMM2012, pp. 220-30.

[25] P. Resa, V. Buckin, Ultrasonic analysis of kinetic mechanism of hydrolysis of cellobiose by beta-glucosidase, ANAL BIOCHEM2011, pp. 1-11.

[26] M. Lenz, M. Bock, E. Kühnicke, J. Pal, A. Cramer, Measurement of the sound velocity in fluids using the echo signals from scattering particles, Ultrasonics2011.

Table 1 Example for two measured series of overtones and the result of the resonator evaluations at 21 °C and 27 °C, respectively. The variables z_L/z_T and f_L are obtained solving equation 4 and Matlab® fmincon using the overtones described in this table and f_T = 9313367.457 Hz and σ = 1.2

Overtones at 20,5 °C	**Overtones at 27°C**
F_{71} = 7523461.503	F_{71} = 7608700.488
F_{72} = 7628932.188	F_{72} = 7715278.362
F_{73} = 7734287.157	F_{73} = 7821794.367
F_{74} = 7839628.702	F_{74} = 7928280.114
F_{75} = 7944961.607	F_{75} = 8034716.200
F_{76} = 8049974.766	F_{76} = 8140817.320
F_{77} = 8155219.156	F_{77} = 8247131.579
F_{78} = 8260099.561	F_{78} = 8352800.032
F_{79} = 8365144.642	F_{79} = 8458692.132
z_L/z_T = 0.0796794	**z_L/z_T = 0.0852844**
f_L = 106073.43123	**f_L = 107290.85264**

Table 2 Calculated fundamental frequencies (f_L) for six measurements with ten resonance peaks, respectively with corresponding mean, standard deviation and variation coefficient.

series	fundamental frequency of the liquid-loaded cavity f_L [Hz]										mean c_L	std	var. coefficient
21°C	106112,4	106111,7	106110,2	106109,8	106110,6	106108,6	106111,6	106112,1	106117,7	106121,6	106112,63	3,76	3,55E-05
22°C	106326,3	106327,4	106326,0	106325,5	106326,3	106324,4	106327,8	106328,3	106334,0	106341,5	106328,75	4,93	4,63E-05
23°C	106537,2	106536,1	106534,3	106533,7	106535,0	106533,1	106536,4	106537,2	106542,7	106551,3	106537,70	5,19	4,87E-05
25°C	107428,2	107427,1	107426,4	107425,7	107427,2	107428,3	107427,6	107432,3	107434,3	107437,0	107436,97	3,59	3,34E-05
26°C	107043,5	107040,7	107041,4	107040,5	107040,4	107041,4	107039,8	107043,7	107046,1	107049,4	107042,70	2,87	2,68E-05
28°C	107140,8	107139,2	107138,3	107137,7	107137,9	107139,2	107138,5	107141,8	107142,9	107145,4	107140,17	2,39	2,23E-05
											mean std	3,79	

Table 3 Baseline-corrected calculated fundamental frequencies (f_L) for six measurements with ten resonance peaks, respectively with corresponding mean, standard deviation and variation coefficient.

series	fundamental frequency of the liquid-loaded cavity f_L [Hz]										mean c_L	std	var. coefficient
21°C	106112,7	106112,7	106112,3	106112,6	106113,7	106111,5	106113,4	106111,6	106113,6	106112,3	106112,63	0,71	6,73E-06
22°C	106329,3	106329,9	106328,9	106329,1	106330,5	106328,6	106330,9	106328,7	106329,6	106329,8	106329,53	0,73	6,83E-06
23°C	106538,8	106538,5	106537,8	106538,2	106540,1	106538,0	106539,9	106537,7	106538,2	106539,4	106538,66	0,83	7,78E-06
25°C	107435,2	107435,3	107435,2	107434,6	107435,5	107435,5	107433,1	107435,6	107434,9	107434,3	107434,93	0,73	6,75E-06
26°C	107044,0	107042,3	107044,0	107043,7	107043,9	107044,6	107042,1	107044,2	107044,0	107043,8	107043,67	0,77	7,20E-06
28°C	107140,3	107140,2	107140,3	107140,2	107140,3	107140,9	107139,2	107140,9	107140,1	107140,3	107140,27	0,45	4,19E-06
											mean std:	0,70	

Chapter

4

Measurement and mathematical modelling of the relative volume of wheat dough during proofing

M. Stanke, V. Zettel, S. Schütze, B. Hitzmann,

Journal of Food Engineering, 131: 58-64

Abstract

Dough is a complex system where yeast cells produce carbon dioxide during the leavening process. Mechanistic models were fitted to measurements of the relative volume of wheat dough during proofing obtained from a Rheofermentometer. The measurements are carried out using 2 and 4% of fresh yeast and proofing temperatures of 28, 32 and 35 °C. The free parameters were the viscosity, a specific CO_2 production rate and the number of bubbles. The following assumptions were made: spherical bubbles in the dough liquid, considered to behave as a Newtonian liquid, the applicability of the Bernoulli and ideal gas equations as well as the diffusion theory. The relative volume during proofing was simulated with an average percentage error less than 0.5% and the dependency between volume expansion and calculated CO_2 production rate was obtained with an R^2 of 0.88.

***Keywords**: Numerical simulation, relative dough volume prediction, proofing, CO_2 production rate, Rheofermentometer, particle swarm optimization*

1 Introduction

Proofing of dough is a key step in the production of voluminous baked goods. However dough is a complex system where yeast cells are used in the leavening process to produce carbon dioxide for the typical sponginess and fluffiness of the final product. Variances in the leavening time are common and can possibly lead to non-optimal capacity utilization in bakeries or products with a minor volume. The optimal proofing time can only be determined by specially trained and experienced operators. Often baking improvers are added to standardize dough and thus minimize variances. Supervising this process by calculating the production rate, and possibly predicting the optimal proofing time as early as possible during the fermentation, could strongly assist this process and avoid non optimal leavened dough. A computational assisted method using mathematical process models could also be integrated in computer assisted optimization of bakeries as described by Hecker et al. (Hecker et al., 2013).

One of the first attempts to model the leavening process was presented by de Cindio and Correra (de Cindio and Correra, 1995). They introduced a complex model, including the kneading and baking process. The different metabolic pathways like lactic acid and ethanol production were included to calculate pH and acidity. Later Shah et al. (Shah et al., 1998) presented a more simple model, based on classical one-component (carbon dioxide) diffusion theory for the rising gas bubbles. The model described a single representative bubble with a mean bubble radius. The carbon dioxide concentration available in the dough was considered to be constant at its maximum solubility, but the influence of the viscosity was not considered. Chiotellis and Campbell (Chiotellis and Campbell, 2003b) extended the model from Shah et al. with a Michaelis-Menten-like time-dependent CO_2

production rate, allowing the carbon dioxide concentration in the dough liquid to increase over time. They further extended the model by using a bubble distribution rather than one mean bubble size. Córdoba (Córdoba, 2010) also considered viscous effects and the Michaelis-Menten-like kinetic modification. However, by choosing a Michaelis-Menten constant of zero, it resulted in a constant CO_2 production rate. He also performed model simulations to fit the model to actual measured data using four different dough recipes.

Romano et al. (Romano et al., 2007) described the variation of dough volume as a function of time, using the more often used Gompertz model derived from the description of bacterial growth in pH-controlled batch cultures. Bikard et al. (Bikard et al., 2008) presented a 3D numerical simulation approach, modeling a 1 cm^3 of dough sample using the finite element method.

Many individual properties of dough are already known and have been often described. For example Upadhyay et al. (Upadhyay et al., 2012) described rheological characteristics and the microstructure of dough. Zúñiga and Le-Bail (Zúñiga and Le-Bail, 2009) presented results of heat transfer measurements in the dough, showing gradients towards the core. Also pressure inhomogeneity can be observed as described by Grenier et al. (Grenier et al., 2010). In situ methods like the X-ray tomography give insights into the actual bubble growth as described by Babin et al., Bellido et al. and Turbin-Orger et al. (Babin et al., 2006; Bellido et al., 2006; Turbin-Orger et al., 2012). They presented changes of dough porosity during the leavening process (an increase in porosity from 0.1 to 0.7) as well as coalescence phenomena. The phenomenon of coalescence was also discussed by Mills et al. (Mills et al., 2003). They showed the appearance of coalescence after a certain amount of time based on model simulations derived from Shah et al. (Shah et al., 1998). The formation of new bubbles was neglected due to the very high pressure that needs to be overcome according to the Young Laplace law. By introducing an anisotropy factor (ratio of the major to the minor axis of an ellipsoid), Bellido et al. (Bellido et al., 2006) showed that only ellipsoid bubbles were present. They showed that the bubbles size was distributed according to a log-normal distribution with a geometric mean of 50 µm radius. The mean of the bubble radii varied in publications between 16 µm (Upadhyay et al., 2012), 110 µm (Turbin-Orger et al., 2012), 180 µm (Babin et al., 2006) and 300 µm (de Cindio and Correra, 1995).

For the mechanistic mathematical description of the volume evolution during the proofing process, certain assumptions are necessary: only spherical bubbles are present which are evenly distributed in liquid dough and which do not change in number; the Bernoulli, the Henry and the ideal gas law as well as the diffusion theory can be applied; the CO_2 is the only diffusing substance. The temperature is the same all over the dough. One representative bubble is simulated.

As the statistician George Box once taught: “Since all models are wrong the scientist cannot obtain a “correct” one…yet he can derive results which match, to a useful approximation, those found in the real world ” (Box, 1976), hence the obvious inadequacies of the model were accepted. Certain modifications to the model used by Córdoba (Córdoba, 2010) are introduced such as a factor for the specific CO_2 production rate as well as the yeast concentration The model is fitted to measurements, using experiments at different temperatures and different amounts of yeast to show the prediction accuracy of the modified model. The measurements are carried out in a specialized proofing chamber called Rheofermentometer, restricting the dough to develop its volume only in one dimension and giving precise results for the actual dough volume. The model is proposed as a possible monitoring system to supervise the dough leavening process through the indirect measurement of the specific CO_2 production rate.

Table 1 Nomenclature of all parameters and variables with corresponding symbol and value.

Name	*Symbol*	*Unit*	*Value*
Parameters (Constant)			
Diffusion coefficient	D	m^2/s	Equation 6
Herny Constant	H	J/kmol	Equation 5
Pressure	p	Pa	10^5
Ideal gas constant	R_g	J/kmol K	8.314
Surface tension	γ	J/m^2	0.04
Water fraction	X_w	1	0.4
Amount of substance	n	kmol	
Radius	R	m	
CO_2 dough concentration	C_D	$kmol/m^3$	
CO_2 equibrillum concentration	C*	$kmol/m^3$	
Dough volume at time t	V(t)	m^3	
Gas volume	V_{gas}	m^3	
Relative dough volume	$V_{rel}, \hat{v}_{rel}$	1	
Volume of gas free dough	$V_{Gas\ free}$	m^3	
Piston height at time t	h(t)	mm	
Porosity	$P, \hat{P}$	1	0.1 – 0.7
Parameters (Due to the experimental conditions)			
Temperature (experiments)	T	°C	28 , 32, 35

Temperature (equations)	T	K	
Initial Bubble Radius	$R_0=R_{t=0}$	m	3^{-4}
Biomass (fresh yeast)	X	g	4, 8
CO_2 production rate	q_{CO2} X	kmol/m^3/s	
Variables			
Viscosity	η	Pa s	
Specific CO_2 production rate	q_{CO2}	1/s	
Number of bubbles per volume	N_b	1/m^3	

2 Material and Methods

The dough was produced with commercial wheat flour (196.82 g, Schapfenmühle, type 550: 0.51 – 0.63% mineral supplements in dry matter, 11.87% moisture content), water (119.18 g), salt (4 g) and commercial yeast (4 g and 8 g, Omas Ur Hefe, Fala, Germany, four 41 g units taken from one batch and stored in a fridge at 7 °C for 2 days) in a mixer (N50, Hobart GmbH, Germany).

Mixing time and water temperature were kept constant at 4 min and 32 °C, the temperature of the prepared dough ranged between 23.8 °C and 27.8 °C depending on the room temperature. After mixing, 200 g of the dough was hand rounded on a worktop, until the dough formed a ball. Subsequently the dough was incubated for 80 min in a Rheofermentometer (Chopin, France) at temperatures of 28, 32 and 35 °C, charged with 1 kg weight.

The six different experimental conditions were repeated four times; therefore 24 individual experiments were performed in total.

3 Calculations

3.1 Model calculations

The differential equation system for the dough modeling is based on the work of Córdoba (Córdoba, 2010). However, only first order differential equations were used. The increasing bubble radius over time is described by Equation 1.

$$\frac{dR}{dt} = \frac{3nR_gT}{16\pi R^2\eta} - \frac{pR}{4\eta} - \frac{\gamma}{2\eta} \quad (1)$$

R is the bubble radius, n the amount of substance in the bubble, R_g the gas constant, T the temperature, □ the viscosity, p the pressure in the liquid dough, and □ the surface tension. The

change of CO_2 concentration in the liquid dough is presented in Equation 2. As distinguished from Córdoba (Córdoba, 2010) where the CO_2 production rate was modeled by a Michaelis-Menten-like kinetic, here it is described by the product of a specific CO_2 production rate q_{CO_2} and the yeast biomass X. The decrease of the CO_2 concentration in the liquid dough (last term of Equation 2) is obtained by the total amount of CO_2 diffusing in the overall N_b existing bubbles per unit volume of gas-free dough. The exchange area was determined from the sphere radius R.

$$\frac{dC_D}{dt} = q_{CO_2}X - 4N_b D\pi R(C_D - C^*) \tag{2}$$

D is the diffusion coefficient, C_D the carbon dioxide concentration in the dough, C* the carbon dioxide concentration, which is in equilibrium with its partial pressure in the bubble. Equation 3 represents the increase of the amount of substance in a bubble due to its concentration difference in the liquid and the gas phase.

$$\frac{dn}{dt} = 4D\pi R(C_D - C^*) \tag{3}$$

According to Shah et al. (Shah et al., 1998) Henrys law can be applied in the form of Equation 4.

$$C^* = \frac{p}{H}\left(1 - \left(\frac{R_0}{R}\right)^3\right) + \frac{8\gamma}{HR}\left(1 - \left(\frac{R_0}{R}\right)^2\right) \tag{4}$$

The temperature dependence of the Henry's constant was used as described by Chiotellis and Campbell (Chiotellis and Campbell, 2003a) for a carbon dioxide-in-dough system (Equation 5).

$$H = 60{,}000\ \frac{J}{kmol \cdot K} \cdot T + 900{,}000\ \frac{J}{kmol} \tag{5}$$

The temperature dependence of mass diffusion coefficient D was considered according to the Chemical Engineers Handbook (Reid, 1974) as

$$D = 1.77 * 10^{-9} \cdot X_w \cdot \frac{T}{298\ K}\frac{m^2}{s} \tag{6}$$

with a water fraction of $X_w = 0.4$.

The specific CO_2 production rate, viscosity and the number of bubbles were used as free parameters. Table 1 gives an overview of the parameters and variables used in the model equations as well as the units and their common values.

To solve the differential equation system the initial conditions were:

$R(t=0) = R_0$,

$C_D(t=0) = 0$,

C*(t=0) = 0 ,

$$n(t=0) = \frac{2\pi {R_0}^2}{3R_g T}(2pR_0 + 4\gamma) \quad (7)$$

3.2 Solving the differential equation system

The system of ordinary differential equations of first order was solved using Matlab (R2012a, The MathWorks Inc., Natick, Massachusetts USA). The Euler method was used with a step size of Δt = 1 s for the integration. For the parameter optimization, a generic particle swarm optimizer (PSO) was applied as described by Kennedy and Eberhart (Kennedy and Eberhart, 1995) with a local convergence parameter (c_1 = 1.2) and a global convergence parameter (c_2 = 1.2).

The particle swarm optimization is a metaheuristic approach, i.e. a method to find optimal solution candidates within a given search space. It roots in the idea of an animal swarm on its search for food. They spread out and if one individual finds a good spot, the swarm will follow. The movement of each single particle is random to some extent, but the swarm as a whole moves towards the optimum position. This concept is adapted to the minimization of a function $y = f(x)$, where f is a quality function to be minimized and x represents the parameters determining the position of a particle in the n-dimensional search space. Each particle owns a velocity vector which determines the direction and speed of the particle. The best position every particle has ever reached and the overall best position achieved by all members of the particle swarm is attached to each single particle. Every iteration of the optimization algorithm the new position of all particles is calculated by changing the present velocity in the direction of the best position for both each single particle and the entire swarm for a specific time step. A random component is applied during the change of velocity. To improve convergence, the velocity is reduced with increasing iterations. The PSO is a global optimization algorithm that does not get stuck in local optimal solutions. It does not need knowledge of the quality function to be optimized, unlike gradient decent algorithms. Furthermore it is able to cover large solution spaces.

To calculate the free parameters (specific CO_2 production rate, viscosity and number of bubbles) as quality function the method of least squares was used, where the difference between measurement and simulation of the relative dough volume was compared (Equation 8).

$$\mathrm{F}\left(q_{\mathrm{CO}_2}, \eta, N_b\right) = \sum_{i=1}^{n}\left(V_{rel,i} - \hat{V}_{rel,i}\right)^2 + (P_n - \hat{P}_n)^2 = min \quad (8)$$

To ensure agreement between the simulated and measured gas volumes, a constraint was applied. The porosity $\hat{P}$ was calculated from the relative volume, where an initial porosity of P(t=0) = 0.1 was assumed at the beginning of the fermentation, and for $\Delta V = V(t) - V(t=0)$ was used.

$$\hat{P} = \frac{V_{gas}}{V(t)} = \frac{P(t=0)\cdot V(t=0)+\Delta V}{V(t)} = \frac{\hat{V}_{rel}(t)-P(t=0)-1}{\hat{V}_{rel.}(t)} \tag{9}$$

The porosity P was calculated from the volume occupied by the bubbles and the relative measured volume.

$$P = \frac{\frac{4}{3}\pi R(t=n)^3 N_b \cdot V_{Gas\ free}}{V(t=n)} \tag{10}$$

with V_{rel} as the relative volume as described in Equation 11 and $V_{Gas\ free}$ as the gas free dough volume described as 0.9 V(t=0).

$$V_{rel}(t) = \frac{V(t)}{V(t=0)} = \frac{h(t)}{h(t=0)} \tag{11}$$

$$\hat{V}_{rel.}(t) = [R(t)/R_0]^3 \tag{12}$$

Here h(t) is the height measurement of the piston performed by the Rheofermentometer.

For each particle (i.e. for each corresponding value of the specific CO_2 production rate, viscosity and number of bubbles) the system of differential equations was solved and $F\left(q_{CO_2}, \eta, N_b\right)$ was calculated. This was performed in each iteration until the maximum was reached. The parameter estimation for one leavening curve took 2 min with 150 particles and a maximum of 300 iterations on a computer with a 2.4 GHz processor.

3.3 Calculation of CO_2 production rate using pressure measurements by the Rheofermentometer

Aside from the dough development curve, the Rheofermentometer also measures the pressure in the proofing chamber. These values were used to calculate the amount of produced CO_2. Since the integral of the pressure measurements is proportional to the amount of CO_2 produced,the amount of CO_2 and the production rate were calculated using the ideal gas law $\rho\, V = n\, R_g\, T$ ..

4 Results and Discussion

4.1 Data pre-processing

In Figure 1 a typical result from a Rheofermentometer dough height measurement is shown. The solid line is the result of the change of the sensor height value resulting in the development curve. The development curve shows a distinct lag phase which can be caused by multiple effects. Examples include: CO_2 dissolving in the liquid phase before evaporation in the gas bubbles; the typical lag phase, known from population dynamics, due to adaption in the new environment; the dough relaxation after the kneading process. After a certain amount of time the height evolution reduces asymptotically towards a maximum. This is most likely because of bubble coalescence and associated loss in dough stability (Bellido et al., 2006; Penner et al., 2009; Romano et al., 2007; Shehzad et al., 2010).

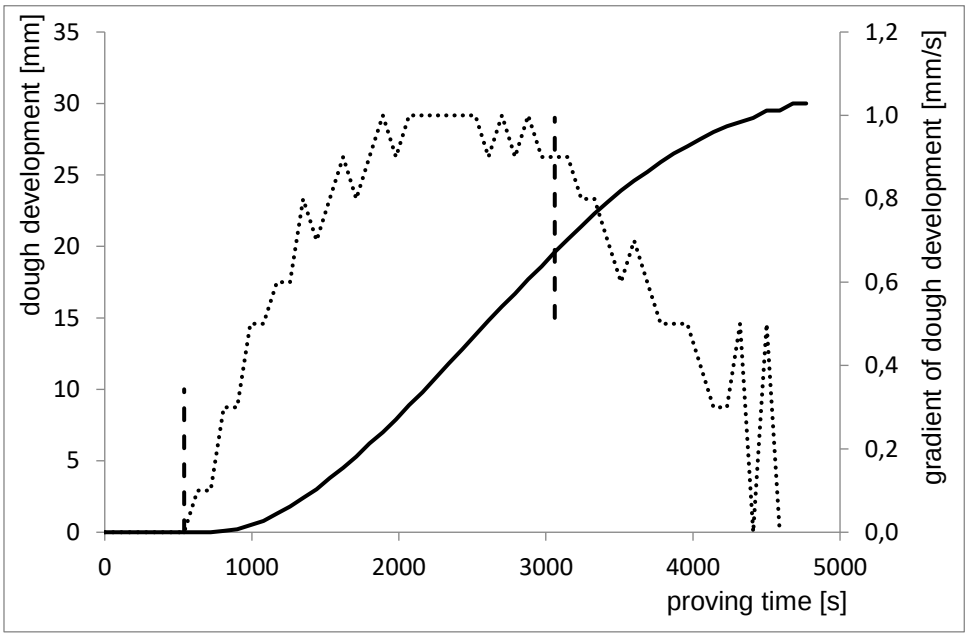

Figure 1 Typical curve of a Rheofermentometer measurement dough development (solid line). On the second axis the gradient of the dough development curve is shown (dotted line). The vertical dashed lines are representing the points where the data were cut for the following evaluation.

Since the description of a lag phase as well as saturation is not included in the mechanistic model presented, pre-processing steps are required. Therefore, only data points for the modeling after the end of the lag phase indicated by a gradient greater than 0 (left vertical dashed line in Figure 1) were used. After the gradient decreased (right vertical dashed line in Figure 1) the remaining data points were discarded. All measurements were pre-processed according to this method.

4.2 Pre-processed experimental data

In Figure 2 the pre-processed results of the experiments, condensed to a mean curve with corresponding standard deviation within the groups of same amount of yeast and at the same temperature are presented. Although the dough samples were carefully prepared, variations within the same experimental setup can be seen.

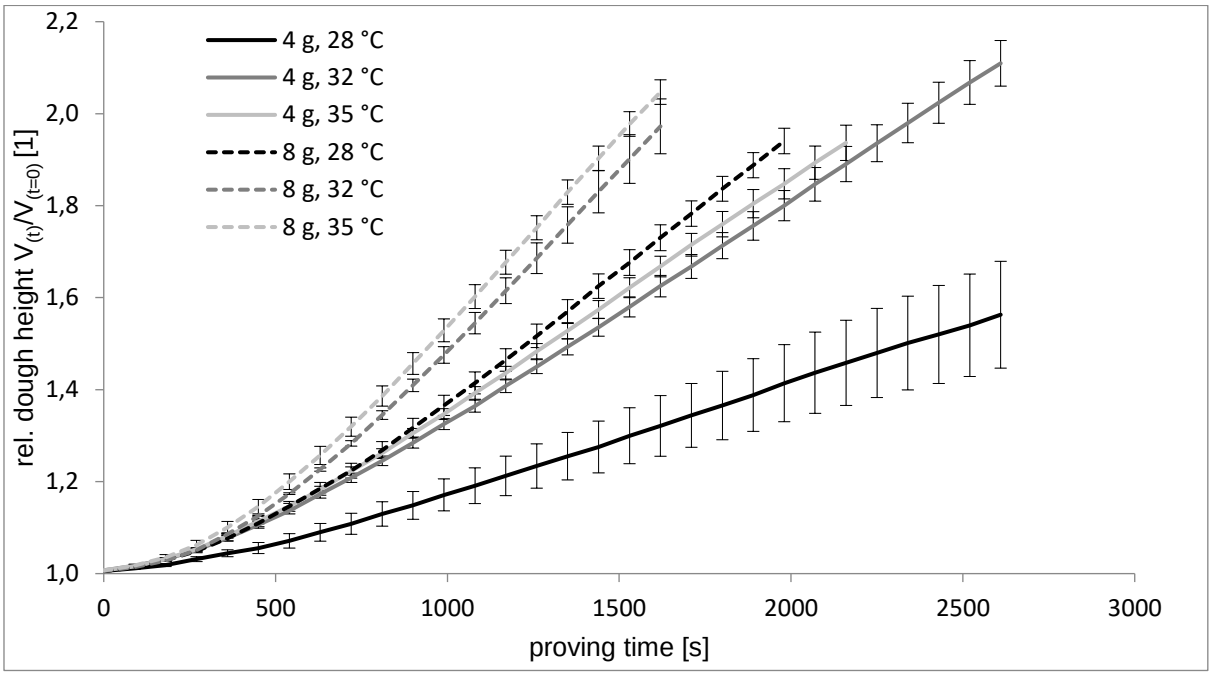

Figure 2 Mean curves of the six different experimental conditions in the Rheofermentometer proofing chamber for 4 and 8 g of fresh yeast with 28, 32 and 35 °C proofing temperature, respectively. The error indicator bars are describing the respective standard deviation within the corresponding group.

Nonetheless each experimental setup has a characteristic mean curve that can be clearly separated from other setups. As expected, the higher the amount of yeast cells and the higher the temperature, the higher the relative dough volume increase, indicating the yeast cells produce more CO_2. Calculating the porosity according to equation 9, all dough samples show the characteristic of decreasing gradient of the dough height evolution at a porosity of 0.53 ± 0.05. This happened at different times during the proofing. The maximal porosity at the end of leavening for all the various dough was around 0.65 ± 0.02, which is in agreement with the described porosity of 0.1 – 0.7 during the leavening process (Babin et al., 2006; Bellido et al., 2006). A reference time t=1620 s was chosen to give measurement volumes, referenced as $V_{(1620)}$ to compare the volumes of all 24 experiments.

In Figure 3 the obtained relative volumes $V_{(1620)}/V_{(t=0)}$ with respect to different temperatures are shown. The difference between the individual measurements carried out with 4 g of fresh yeast and 8 g of fresh yeast can clearly be distinguished. Also a certain temperature dependency can be seen, especially distinct for the measurements carried out at 28 °C. The experiments with 4 g of yeast at 28 °C and 8 g of yeast at 32 °C show the greatest deviation. However one experiment carried out with 8 g of yeast and at 32 °C seems to be an outlier ($V_{(1620)}/V_0$= 2.06).

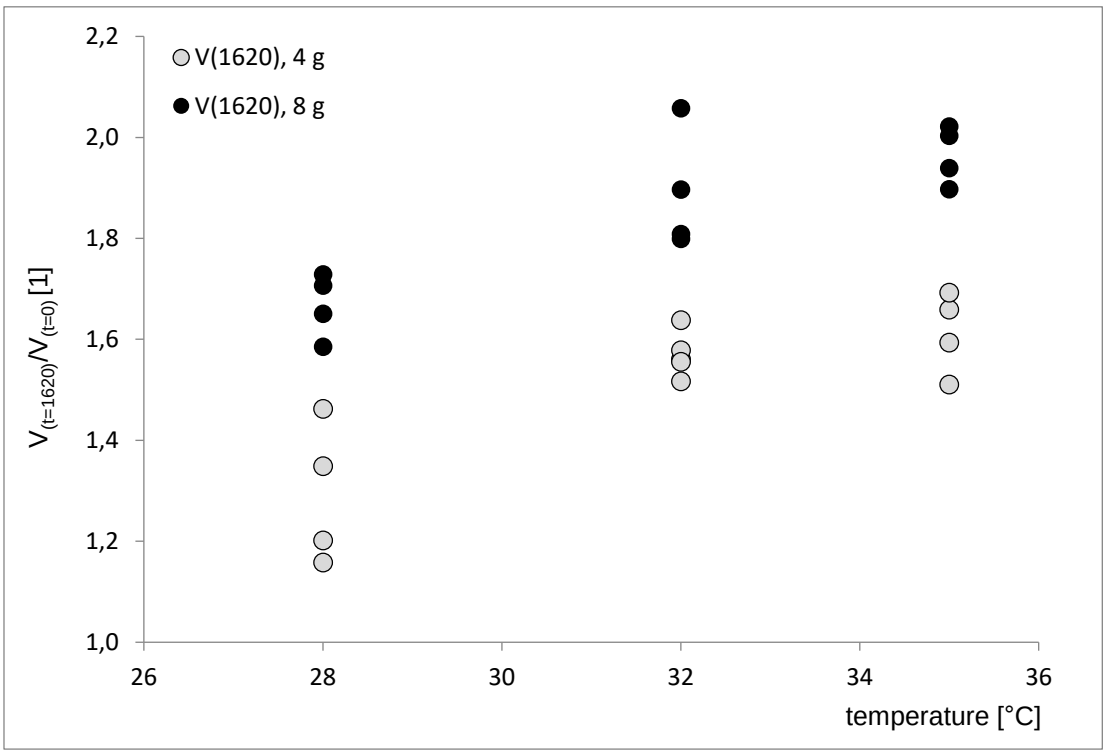

Figure 3 Measured relative volume of the dough after 1620 s of proofing time with respect to the proofing temperature.

In Table 2 the percentage error for the individual experiments within the different conditions are presented. Excluding all the experiments with 4 g of yeast at 28 °C and the one experiment with 8 g of yeast at 32°C the average percentage error is 10.6%, which seems to be acceptable.

Table 2 Percentage error of the V(t=1620) values of the experiments

Percentage error of	**28 °C**	**32 °C K**	**35 °C**
V(t=1620) from experiment 4 g yeast	39.47 %	9.59 %	9.06 %
V(t=1620) from Experiment 8 g yeast	10.75 %	24.90 %	14.84 %

Although the production of fresh yeast is highly standardized, as can be seen in Birch et al. (Birch et al., 2013), where different commercially available fresh yeast samples were examined, variation of the dough leavening cannot be excluded. The difference between batches of dough highly depends on environmental conditions, especially the temperature. The experiments presented in this contribution showed up to a 4 °C difference in the temperature of the kneaded dough. This was mainly caused by fluctuating room temperatures. The temperature gradient in the dough also affects the leavening process. Furthermore, the process of hand rounding influenced the inner tension of the dough sample, the distribution of gas bubbles and their size distribution. The conditions of the raw materials particularly influences the leavening behavior as can be seen e. g. in Sahlström et al. (Sahlström et al., 2004). The dough samples showed the variation in their behavior due to the combination of all these effects,.

4.3 Calculation results

An example of measured and simulated values of the relative volume of the dough is shown in Figure 3, presenting the relative volume of one measurement at 32 °C with 4 g yeast. The percentage error of the simulation fit to the measured data is less than 0.5%.

The results obtained from the parameter estimation can be seen in Table 3 as mean values of the free model parameters specific CO_2 production rate (q_{CO2}), viscosity (η) and the number of bubbles (N_b) with its standard deviation. A sensitivity analysis was performed to determine the quality of the parameters. The relative values with respect to the optimal values of the parameters were varied between 0.5 and 1.5. The sensitivity of a parameter was then determined by the values of the quality function. A high increase of the values of the quality function indicates a high sensitivity of the parameter whereas a low increase indicates a poor determination of the parameter during fitting. In

Figure 4 the results of the sensitivity study are presented. The specific CO_2 production rate and the number of bubbles are the free parameters with the highest sensitivity while the viscosity has a much smaller impact compared to the other two.

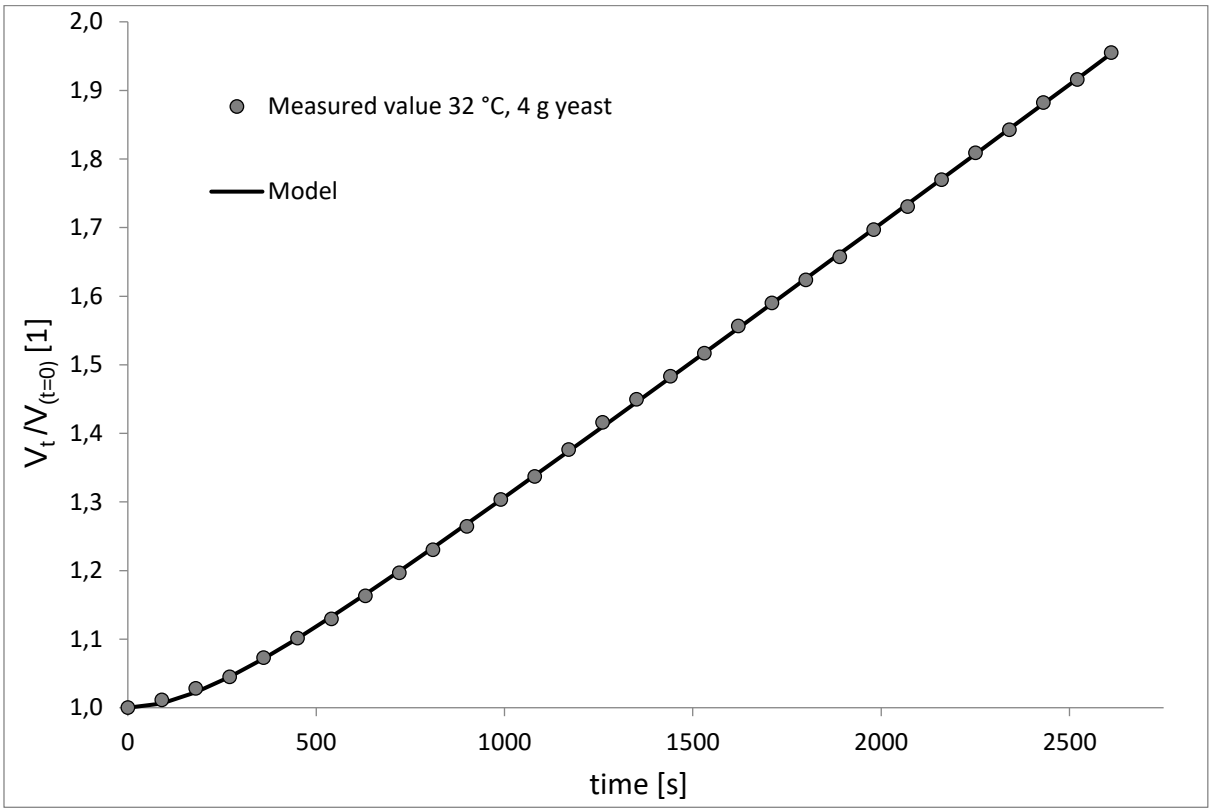

Figure 4 Exemplary dough development (relative volume) measurements for 32 °C and 4 g of yeast as well as the result of the model simulation fit (solid line). The square sum of error of the model fit is <0.05.

This is nonetheless in accordance with the standard deviation presented in Table 3. The experimental variation is inherent in the error value of Table 3 whereas the values of the quality function represent the influence of the parameters for the description of one experiment by the model. As it can be seen in Figure 4, the quality function is asymmetrical. Smaller values for the parameters, number of bubbles and the viscosity result in a higher increase in the quality function compared to higher values. For the specific CO_2 production rate the behavior is reversed.

Table 3 Mean values of the results obtained from the parameter estimation of the free parameters with corresponding standard deviation and percentage error. The specific CO_2 production rate is discriminated between the different temperatures. For the viscosity and number of bubbles per volume the mean values over all experiments are presented.

Free parameter		**Mean value**	**Standard deviation**	**Percentage error %**
Specific $C0_2$ production rate [1/s]	28 °C	2.31×10^{-6}	0.56×10^{-6}	24.1
	32 °C	3.54×10^{-6}	0.56×10^{-6}	15.8
	35 °C	3.54×10^{-6}	0.45×10^{-6}	12.9
Viscosity [Pa s]		3.92×10^{7}	3.18×10^{7}	81.0
Number of bubbles [$1/m^3$]		3.15×10^{9}	0.41×10^{9}	13.1

The viscosity is not expected to change due to the dough formulation and treatment. However the temperature variation and the increased sheer stress, due to the higher CO_2 production rate, could influence the viscosity values. The low sensitivity of the viscosity of the dough is also reflected in the calculation results. Here the majority is in the same dimension with a mean value of 3.92×10^7 Pa s and a standard deviation of $\pm 3.18 \times 10^7$ Pa s.

The calculated CO_2 production rates are presented in Figure 5 with respect to temperature and yeast concentration. Similar to the results presented in Figure 3, the difference between 4 and 8 g of yeast can be distinguished. A clear linear dependency between the actual reached relative volume at 1620 s and the calculated production rate is seen (Figure 6) with a coefficient of determination of $R^2 = 0.88$. This indicates that the calculated production rate is in good agreement with the measurements and capable of representing the actual rate of leavening. Figure 7 is obrained by plotting the CO_2 production rates calculated from the CO_2 measurements by the Rheofermentometer against the results from the model fit. As seen from the trendline the Rheofermentometer data are proportional to the model data with a small intercept. Therefore the systematic deviation is not absolute but relative. However the correlation is significant, with a coefficient of determination of $R^2 = 0.93$.

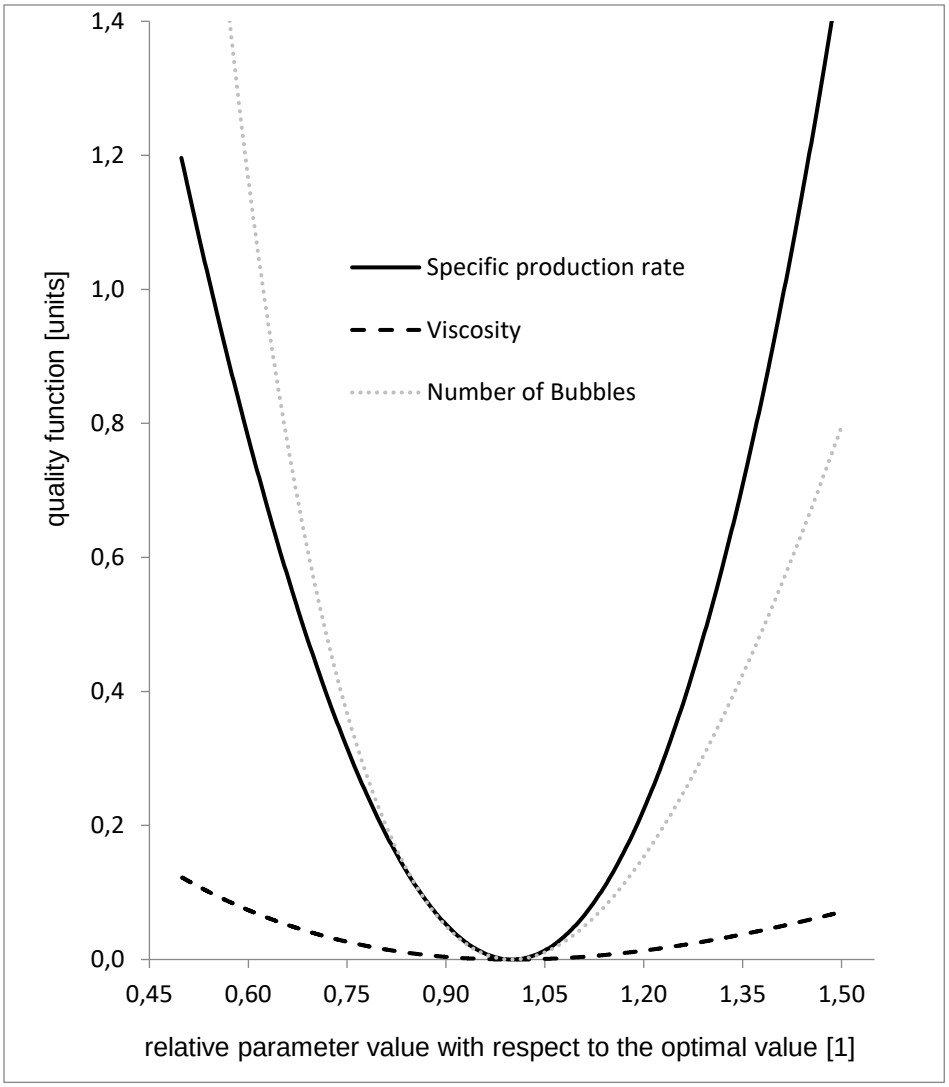

Figure 5 Typical dependence of the quality function on the relative change of free model parameters with respect to their optimal values (experiment 8 g yeast, 32 °C).

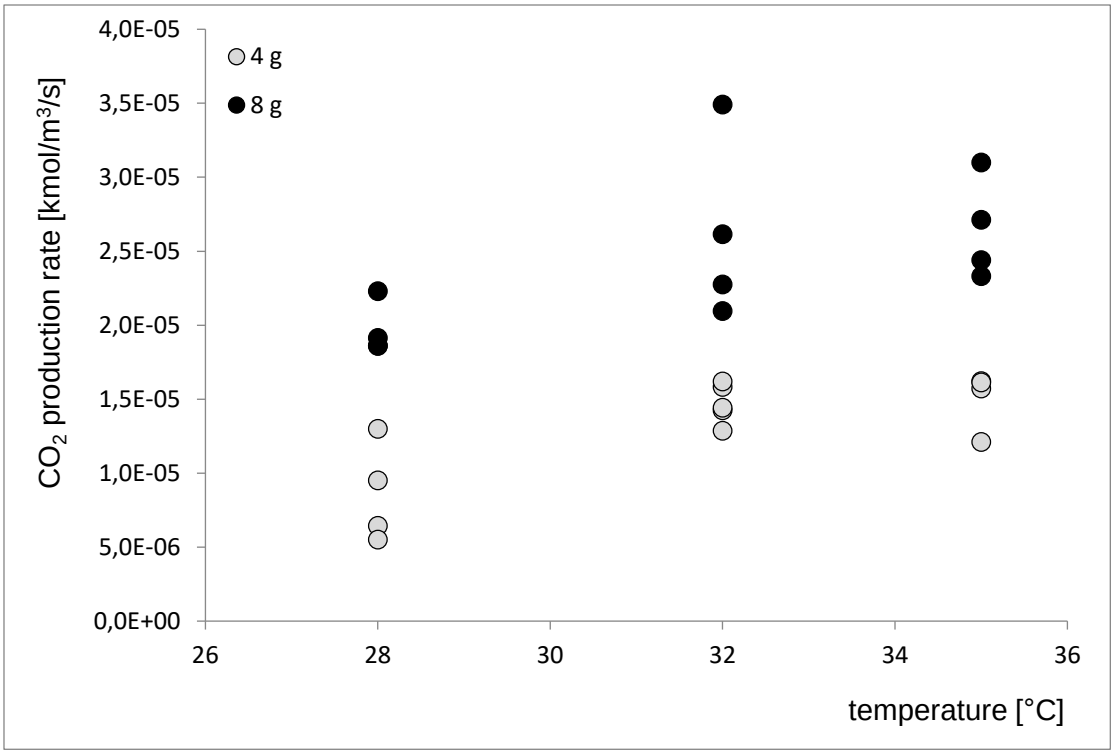

Figure 6 Calculated CO_2 production rate with respect to the proofing temperature for experiments with 4 and 8 g of yeast.

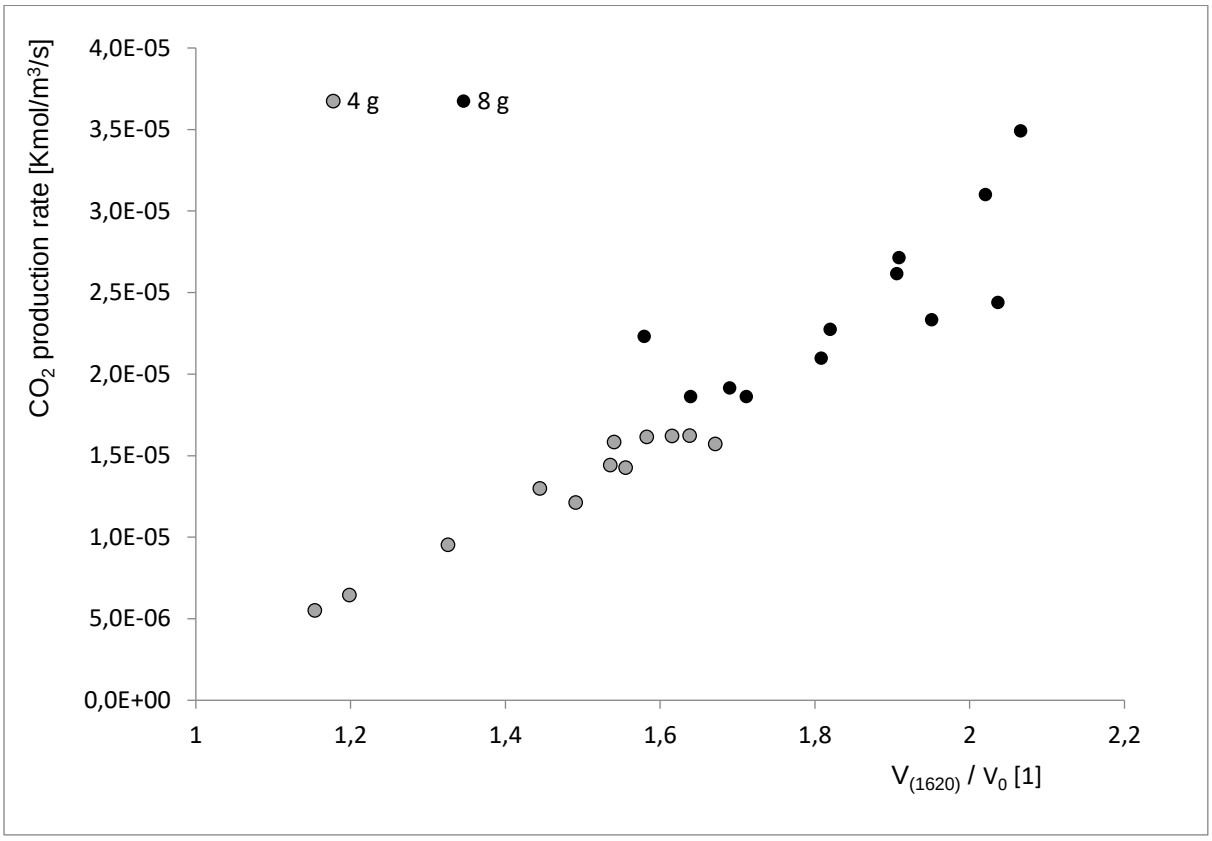

Figure 7 Calculated CO_2 production rate with respect to the relative dough volume after t =1620 s of proofing time.

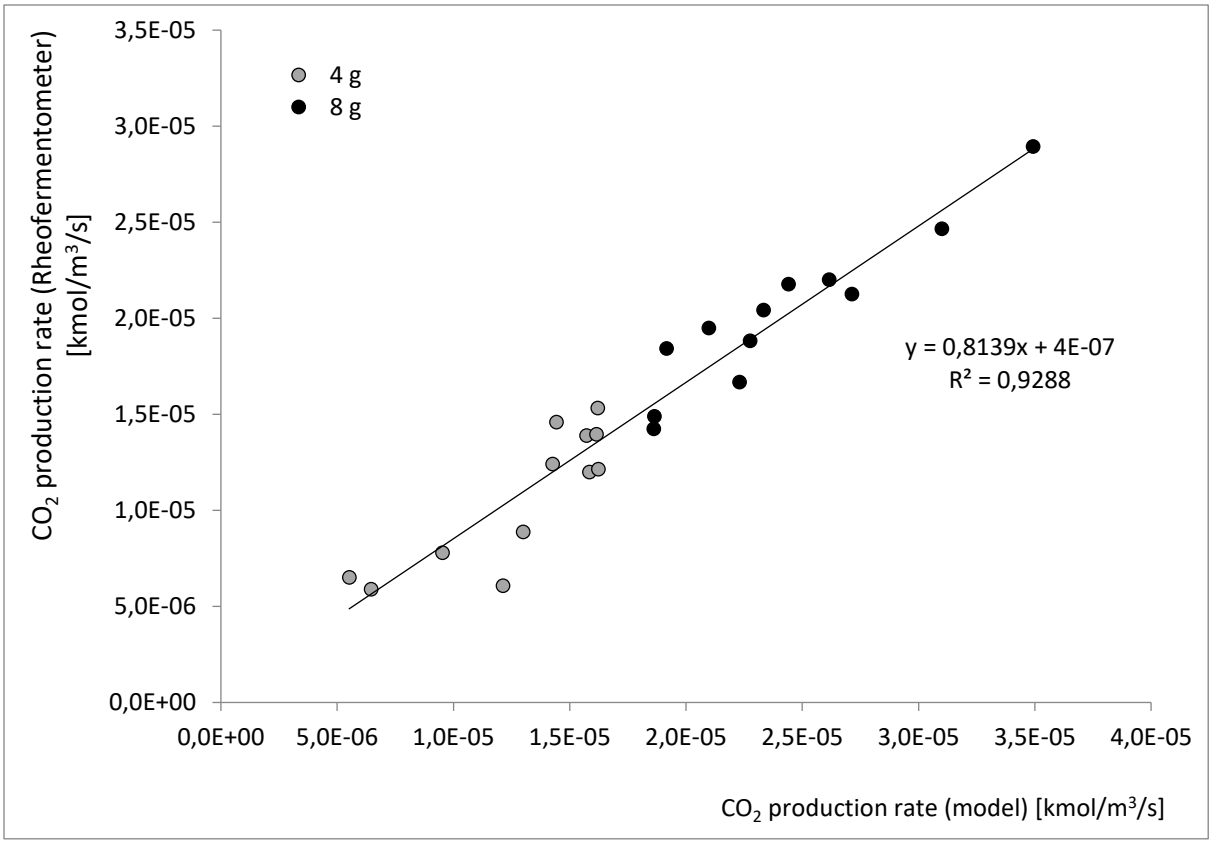

Figure 8 Calculated CO_2 production rate versus the CO_2 production rate calculated from the amount of produced gas measured with the Rheofermentometer

4.4 Number of bubbles and bubble radius

The initial bubble radius was assumed to be 300 µm, which is roughly the value calculated by Córdoba (Córdoba, 2010). According to most of the publications addressing the determination of bubble sizes and its distribution, this is a very high value. However the best model fits and the best prediction was achieved using this bubble size. This is most likely due to the simplification of the bubble shape as a sphere. The surface area of the bubble and the number of total bubbles influence the amount of CO_2 that is diffusing in the bubble (Equation 2 and 3). Here the spherical surface area is not capable of describing this phenomenon with more frequently described radii (≈50 – 180 µm). Using smaller spherical bubbles resulted in no satisfactory model fits as higher errors were obtained and the characteristic evolution of the leavening curve could not be achieved.

The additional constraint, resulting from equations 8 and 9, prohibits unrealistic void volumes and determines the number of bubbles. Here the mean number of bubbles is 3.15 x 10^9 1/m^3 with a standard deviation of 0.41x 10^9 1/m^3. The use of the high bubble radius prevents an accurate simulation of the trajectory of porosity using Equation 10 during the fermentation, but ensures a correct final porosity. The superposition of different sized and shaped bubbles and associated ratio of

bubble surface to volume can be reasonably approximated by a radius of 300 µm, covering the actual substance transfer.

5. Conclusion

The maximum error for the relative volume determination in the experiments were 40% for 4 g of yeast at 28 °C and the minimum error 9% for 4 g of yeast at 35 °C, indicating the variation caused by the yeast and temperature inadequacies for identically prepared samples. This shows the importance of well-trained personnel, the addition of baking improvers to standardize dough and thus minimize these variances or a computational assisted method predicting the optimal time for the leavening process.

Supervising this process by calculating the production rate and possibly predicting when the proofing time is optimal could strongly assist this process, thus avoiding non optimal leavened dough. We demonstrated that the model is able to describe the leavening process by introducing the specific CO_2 production rate as variable and the biomass as parameter. Using different amounts of yeast at different temperatures, the process could be modeled with an average percentage error less than 0.5%. The dependency between the relative volume reached and calculated CO_2 production rate had an R^2 of 0.88. Therefore the model can be used to establish a monitoring system for the leavening process.

6. References

Babin, P., Della Valle, G., Chiron, H., Cloetens, P., Hoszowska, J., Pernot, P., Réguerre, A.L., Salvo, L., Dendievel, R., (2006). Fast X-ray tomography analysis of bubble growth and foam setting during breadmaking. Journal of Cereal Science 43(3), 393-397.

Bellido, G.G., Scanlon, M.G., Page, J.H., Hallgrimsson, B., (2006). The bubble size distribution in wheat flour dough. Food Research International 39(10), 1058-1066.

Bikard, J., Coupez, T., Della Valle, G., Vergnes, B., (2008). Simulation of bread making process using a direct 3D numerical method at microscale: Analysis of foaming phase during proofing. Journal of Food Engineering 85(2), 259-267.

Birch, A.N., van den Berg, F.W.J., Hansen, Å.S., (2013). Expansion profiles of wheat doughs fermented by seven commercial baker's yeasts. Journal of Cereal Science 58(2), 318-323

Box, G.E.P., (1976). Science and Statistics. Journal of the American Statistical Association 71(356), 791 - 799.

Chiotellis, E., Campbell, G.M., (2003a). Proving of Bread Dough I: Modelling The Evolution of the Bubble Size Distribution. Food and Bioproducts Processing 81(3), 194-206.

Chiotellis, E., Campbell, G.M., (2003b). Proving of Bread Dough II: Measurement of Gas Production and Retention. Food and Bioproducts Processing 81(3), 207-216.

Córdoba, A., (2010). Quantitative fit of a model for proving of bread dough and determination of dough properties. Journal of Food Engineering 96(3), 440-448.

de Cindio, B., Correra, S., (1995). Mathematical modelling of leavened cereal goods. Journal of Food Engineering 24(3), 379-403.

Hecker, F.T., Hussein, W.B., Paquet-Durand, O., Hussein, M.A., Becker, T., (2013). A case study on using evolutionary algorithms to optimize bakery production planning. Expert Systems with Applications 40(17), 6837-6847.

Kennedy, J., Eberhart, R., (1995). Particle swarm optimization, *Neural Networks, 1995. Proceedings., IEEE International Conference on*, pp. 1942-1948 vol.1944.

Penner, A., Hailemariam, L., Okos, M., Campanella, O., (2009). Lateral growth of a wheat dough disk under various growth conditions. Journal of Cereal Science 49(1), 65-72.

Reid, R.C., (1974). Chemical engineers' handbook, R. H. Perry and C. H. Chilton (eds.), McGraw-Hill, New York (1973). $35.00. AIChE Journal 20(1), 205-205.

Romano, A., Toraldo, G., Cavella, S., Masi, P., (2007). Description of leavening of bread dough with mathematical modelling. Journal of Food Engineering 83(2), 142-148.

Sahlström, S., Park, W., Shelton, D.R., (2004). Factors Influencing Yeast Fermentation and the Effect of LMW Sugars and Yeast Fermentation on Hearth Bread Quality. Cereal Chemistry Journal 81(3), 328-335.

Shah, P., Campbell, G.M., McKee, S.L., Rielly, C.D., (1998). Proving of Bread Dough: Modelling the Growth of Individual Bubbles. Food and Bioproducts Processing 76(2), 73-79.

Shehzad, A., Chiron, H., Della Valle, G., Kansou, K., Ndiaye, A., Réguerre, A.L., (2010). Porosity and stability of bread dough during proofing determined by video image analysis for different compositions and mixing conditions. Food Research International 43(8), 1999-2005.

Turbin-Orger, A., Boller, E., Chaunier, L., Chiron, H., Della Valle, G., Réguerre, A.L., (2012). Kinetics of bubble growth in wheat flour dough during proofing studied by computed X-ray micro-tomography. Journal of Cereal Science 56(3), 676-683.

Upadhyay, R., Ghosal, D., Mehra, A., (2012). Characterization of bread dough: Rheological properties and microstructure. Journal of Food Engineering 109(1), 104-113.

Zúñiga, R., Le-Bail, A., (2009). Assessment of thermal conductivity as a function of porosity in bread dough during proving. Food and Bioproducts Processing 87(1), 17-22.

Chapter

5

Summary and final remarks

Summary

Biotechnology is an area where precision and reproducibility are vital. This is due to the fact that products are often in form of food, pharmaceutical or cosmetic products and therefore very close to the human being. To avoid human error during the production or the evaluation of the quality of a product and to increase the optimal utilization of raw materials, a very high amount of automation is desired. Tools in the food and chemical industry that aim to reach this degree of higher automation are summarized in an initiative called Process Analytical Technology (PAT). Within the scope of the PAT, is to provide new measurement technologies for the purpose of closed loop control in biotechnological processes. These processes are the most demanding processes in regards of control issues due to their very often biological rate-determining component. Most important for an automation attempt is deep process knowledge, which can only be achieved via appropriate measurements. These measurements can either be carried out directly, measuring a crucial physical value, or if not accessible either due to the lack of technology or a complicated sample state, via a soft-sensor.

First of a review is given to present the scope and problems of PAT tools in biotechnological applications. The process control, especially the closed loop control is requiring the highest amount of process knowledge. The biological component, mostly microorganisms, makes the prediction of these processes exceptionally demanding. The latest approaches to control complex biological processes from various fields are presented. The most basic tool for a control action is a suitable sensor or in the case of bioprocesses a sensor array, delivering vast amounts of process data. Only a minority of the available applications during the reviewed time period was actually applied to real bioprocesses; the majority is based on theoretical applications using simulated (idealized) processes. For closed loop control applications, in the majority of cases a soft-sensor is combined with a PID controller to determine the feeding rate of substrate or the specific growth rate. The reason that soft-sensors got this importance for control purposes demonstrates the lack of direct measurements or its big additional expenditure for robust and reliable on-line measurement systems. The lack of theoretical bioprocess models is often compensated by hybrid systems combining theoretical models, fuzzy logic and/or artificial neural networks methodology. The review is showing that the noble PAT target of a well-known process is still not fully achieved at this level of complexity. The effort to transfer the presented algorithms and the required measurement systems to new applications is still very high. Which leads to the assumption that closed loop control in many bioprocesses will still be a challenge in the near future.

It is, however, clear that frequently suitable sensors are missing in order to measure all important process variables. In the long term, the development of new sensors is necessary to implement

powerful control algorithms. In this thesis, an on-line sensor design based on the measurement of the sonic velocity is presented. The sonic velocity is a material constant which is highly sensitive to changes in the material composition if varying the adiabatic compressibility or density. The aim of the presented sensor design was to detect the slightest changes in the composition of a volume flow, which is why the focus was on the maximum achievable precision and accuracy of the device. As presented these are not only given by the limitations of the individual components but also by the mathematical model and the chosen solution algorithm. The best results could be obtained using only the tip of the group delay time resonant peak; here the standard deviation for the repetitive sonic velocity determination (precision) was $3 \cdot 10^{-4}\,m \cdot s^{-1}$. Secondly and more important for the automation capability a new evaluation method was presented for the determination of the sonic velocity. The accuracy of the device could be improved using a simple polynomial correction to $0.027\,m \cdot s^{-1}$.

It was examined which information the mathematical description of the proofing process provides for the development and application of a soft sensor for a specific biotechnological process in the food sector. The yeast dough is responsible for the desired sponge-like structure of the final bread and therefore a key step to produce baked goods, typical in the Western world. For the mechanistic mathematical description of the change in volume during the fermentation, certain assumptions must be made. Examples are: Supposed spherical bubbles, which are uniformly distributed in the dough adopted as Newton's fluid, and do not alter their number. The Bernulli, Henry and ideal gas law are applicable. In the dough, carbon dioxide is the only diffusing gas and the temperature is the same throughout the dough. In the model a representative bubble is simulated and extrapolated on the whole dough. The model is based on a differential equation system, modeling the expansion of the gas bubbles that get incorporated in the dough during its preparation. The sum of all growing bubbles is causing the dough to increase its volume. By measuring the volume increase over time the specific production rate of CO_2 could be calculated. The maximum error for the relative volume in the experiments was 40 %, indicating the variation caused by the yeast and temperature inadequacies for identically prepared samples. This showcases the importance of well-trained personnel and the complexity of predicting the optimal time for the leavening process. It was demonstrated that the model is able to describe the leavening process by introducing the specific CO_2 production rate as variable and the biomass as parameter. The process could be modeled with an average percentage error less than 0.5 %. The dependency between the relative volume reached and calculated CO_2 production rate had an R^2 of 0.88. Therefore, the model is a candidate to establish a monitoring system for the leavening process.

Final remarks

Even after several years the ideal aim of the PAT initiative is not fully implemented in the industry and in many production processes. On the one hand a lot effort still needs to be put into the development of more general algorithms which are more easy to implement and especially more reliable. On the other hand, not all the available advances in this field are employed yet. The potential users seem to stick to approved methods and show certain reservations towards new technologies.

However, like Max Planck said: “A new scientific truth does not triumph by convincing its opponents and making them see the light, but rather because its opponents eventually die, and a new generation grows up that is familiar with it.” [2]

---

[2] Planck, Max, Wissenschaftliche Selbstbiographie , Mit der von Max von Laue gehaltenen Traueransprache, Johann Ambrosius Barth 3. Auflage Leipzig 1955.

Zusammenfassung

Die Biotechnologie ist ein Wissenschaftsbereich, in dem hohe Genauigkeit und Wiederholbarkeit eine wichtige Rolle spielen. Dies ist der Tatsache geschuldet, dass die hergestellten Produkte sehr oft den Bereichen Nahrungsmitteln, Pharmazeutika oder Kosmetik angehöhren und daher besonders den Menschen beeinflussen. Um den menschlichen Fehler bei der Produktion zu vermeiden, die Qualität eines Produktes zu sichern und die optimale Verwertung der Rohmaterialen zu gewährleisten, wird ein besonders hohes Maß an Automation angestrebt.

Die Werkzeuge, die in der Nahrungsmittel- und chemischen Industrie hierfür zum Einsatz kommen, werden in der Process Analytical Technology (PAT) Initiative zusammengefasst. Ziel der PAT ist die Entwicklung zuverlässiger neuer Methoden, um Prozesse zu beschreiben und eine automatische Regelungsstrategie zu realisieren. Biotechnologische Prozesse gehören hierbei zu den aufwändigsten Regelungsaufgaben, da in den meisten Fällen eine biologische Komponente der entscheidende Faktor ist. Entscheidend für eine erfolgreiche Regelungsstrategie ist ein hohes Maß an Prozessverständnis. Dieses kann entweder durch eine direkte Messung der entscheidenden physikalischen, chemischen oder biologischen Größen gewonnen werden oder durch einen Soft-Sensor. Ein Soft-Sensor kommt zum Einsatz, wenn direkte Messungen auf Grund fehlender Technologie oder durch die Art, in der die Probe vorliegt, nicht möglich sind. Der Stand der Automation von Prozessregelung in der Biotechnologie wird zunächst in einem Review betrachtet, um den Rahmen und die Probleme der PAT Werkzeuge in biotechnologischen Anwendungen zu beschreiben. Die Prozesssteuerung und besonders die Regelung benötigen in diesem Bereich den höchsten Grad an Prozesswissen. Die biologische Komponente, die in den meisten Fällen durch einen Mikroorganismus repräsentiert wird, macht die Vorhersage des Verhaltens dieser Prozesse besonders fordernd. In diesem Review werden die neuesten Ansätze aus unterschiedlichen Bereichen biotechnologischer Prozesse dargestellt. Das grundlegendste Werkzeug für eine Regelung ist ein geeigneter Sensor oder im Fall eines Bioprozesses ein ganzes Array an Sensoren, die große Mengen an Prozessdaten liefern. Nur eine geringe Anzahl der vorgestellten Methoden wurden in realen biotechnologischen Prozessen verwendet. Die meisten Applikationen waren theoretisch und wurden an simulierten (idealisierten) Prozessen erprobt. Für die Regelungsanwendungen kamen in den meisten Fällen eine Kombination aus Soft-Sensor und PID Regler zum Einsatz, um die optimale Rate der Substratzugabe oder die spezifische Wachstumsrate zu bestimmen. Anhand der vermehrten Verwendung von Soft-Sensoren ist zum einen das Fehlen einer direkten Messmethodik ersichtlich und zum anderen der große Aufwand für ein robusteres und zuverlässigeres Messsystem. Da oft hinreichende Bioprozessmodelle fehlen, kommen hybride Systeme zum Einsatz, die theoretische Modelle, Fuzzy - Logiken und / oder künstliche neuronale Netze kombinieren. Es wird klar, dass das

hohe Ziel der PAT Initiative von einem tiefen Prozessverständnis auf dieser Ebene der Komplexität noch lange nicht erreicht ist. Der Aufwand, um die vorgestellten Algorithmen und benötigten Messsysteme auf einen neuen Prozess zu portieren, ist immer noch sehr hoch. Dies lässt den Schluss zu, dass zumindest in naher Zukunft das Regeln von Bioprozessen weiterhin eine Herausforderung bleibt.

Deutlich ist jedoch, dass häufig geeignete Sensoren fehlen, um alle wichtigen Prozessgrößen zu messen. Langfristig ist die Entwicklung neuer Sensoren notwendig, um leistungsfähige Regelungsalgorithmen zu realisieren. In dieser Arbeit wurde ein on-line Sensoraufbau basierend auf der Messung der Schallgeschwindigkeit vorgestellt. Die Schallgeschwindigkeit ist eine Materialkonstante, die hochsensibel von der Dichte und adiabatischen Kompressibilität des Materials abhängig ist. Das Ziel des vorgestellten Sensoraufbaus ist es, kleinste Änderungen der Zusammensetzung eines Volumenstroms zu detektieren. Daher lag der Fokus der präsentierten Arbeit auf der maximal erreichbaren Genauigkeit und Wiederholbarkeit des Sensors. Es wurde gezeigt, dass die Güte der Messung nicht alleine an den Grenzen der verwendeten Komponenten liegt, sondern auch am verwendeten mathematischen Modell und den Auswertealgorithmen. Die besten Ergebnisse konnten erzielt werden, indem nur die Spitze des Gruppenlaufzeitpeaks verwendet wurde. Die Standardabweichung für die wiederholte Schallgeschwindigkeitsbestimmung lag hier bei $3 \cdot 10^{-4}$ m·s^{-1}. Wichtiger jedoch für den Aspekt der Automation ist die Vorstellung einer neunen Auswertung für die absolute Schallgeschwindigkeitsbestimmung. Die Genauigkeit der Messmethode konnte hierdurch durch den Einsatz einer polynomischen Korrektur auf 0.027 m·s^{-1} verbessert werden.

Im Weiteren wurde untersucht, welche Informationen die mathematische Beschreibung der Gare für die Entwicklung und Anwendung eines Soft-Sensors für diesen speziellen biotechnologischen Prozess im Lebensmittelsektor zur Verfügung stellt. Die Gare von Hefeteig ist verantwortlich für die gewünschte schwammartige Struktur des finalen Gebäcks und daher ein Schlüsselschritt für die Herstellung von Backwaren, wie sie in der westlichen Welt typisch sind. Für die mechanistische mathematische Beschreibung der Volumenänderung während der Gare müssen bestimmte Annahmen getroffen werden, im Folgenden einige Beispiele: Angenommen werden kugelförmige Blasen, welche in dem als Newtonsche Flüssigkeit angenommenen Teig gleichmäßig verteilt vorliegen und ihre Anzahl nicht verändern. Das Bernulli-, Henry- sowie ideale Gasgesetz sind anwendbar. In dem Teig ist Kohlenstoffdioxid das einzige diffundierende Gas und die Temperatur ist überall im Teig gleich. In dem Modell wird eine repräsentative Blase simuliert und auf den ganzen Teig hochgerechnet. Dem Soft-Sensor liegt ein Modell zu Grunde, dass auf einem Differentialgleichungssystem basiert. Dieses simuliert die Ausdehnung der Gasblasen, die bei der

Herstellung des rohen Teiges eingetragen werden. Die Summe aller wachsenden Blasen im Teig führt dabei zu einer Erhöhung des Volumens. Durch die Messung der zeitlichen Veränderung des Teigvolumens wird die spezifische Kohlenstoffdioxid Produktionsrate errechnet. Die maximale Varianz des Teigvolumens lag bei 40 %, für identisch hergestellte Proben. Dies ist ein Anzeichen dafür, wie stark dieser Prozess durch die Hefe- und Temperatur Unterschiede bei der Herstellung variiert, obwohl die Proben identisch hergestellt wurden. Dies zeigt die Komplexität der Vorhersage sowie die Wichtigkeit von gut geschultem Personal um den optimalen Zeitpunkt zu bestimmen, um den rohen Teig dem nächsten Prozessschritt zu übergeben. Es konnte gezeigt werden, dass das Modell durch Einführung der spezifischen Kohlenstoffdioxid Produktionsrate als Variable und der Biomasse als Parameter in der Lage ist den Prozess der Gare zu beschreiben. Der Prozess konnte dabei mit einem durchschnittlichen prozentualen Fehler von weniger als 0,5 % simuliert werden. Der Zusammenhang zwischen erreichtem relativem Volumen und der errechneten spezifischen Kohlenstoffdioxid Produktionsrate hatte ein Bestimmtheitsmaß von 0,88. Daher scheint das Modell ein geeigneter Kandidat zu sein, um ein Überwachungssystem für die Gare zu etablieren.

Schlussbemerkung

Zusammengefasst zeigt sich, dass das finale Ziel der PAT Initiative auch nach einigen Jahren des Propagierens weder komplett in der Industrie noch bei vielen Produktionsprozessen angekommen ist. Auf der einen Seite liegt dies mit Sicherheit an der Tatsache, dass noch viel Arbeit in die Generalisierung von Algorithmen gesteckt werden muss. Diese müsse einfacher zu implementieren und vor allem noch zuverlässiger in der Funktionsweise sein. Auf der anderen Seite wurden jedoch auch Algorithmen, Regelungsstrategien und eigne Ansätze für einen neuartigen Sensor sowie einen Soft-Sensors vorgestellt, die großes Potential zeigen. Nicht zuletzt müssen die möglichen Anwender neue Strategien einsetzen und Vorbehalte gegenüber unbekannten Technologien ablegen.

Wie jedoch Max Planck einmal sagte: "Eine neue wissenschaftliche Wahrheit pflegt sich nicht in der Weise durchzusetzen, dass ihre Gegner überzeugt werden und sich als belehrt erklären, sondern vielmehr dadurch, dass ihre Gegner allmählich aussterben und dass die heranwachsende Generation von vornherein mit der Wahrheit vertraut gemacht ist." [1]

---

[1] Planck, Max, Wissenschaftliche Selbstbiographie , Mit der von Max von Laue gehaltenen Traueransprache, Johann Ambrosius Barth 3. Auflage Leipzig 1955.

Appendices

Eidesstattliche Versicherung gemäß §7 Absatz 7 der Promotionsordnung der Universität Hohenheim zum Dr. rer. nat.

1. Bei der eingereichten Dissertation zum Thema:
   „Process Analytical Technology in Food Biotechnology - by means of sensors, signal processing, modelling and process control – „
   handelt es sich um meine eigenständig erbrachte Leistung.
2. Ich habe nur die angegebenen Quellen und Hilfsmittel benutzt und mich keiner unzulässigen Hilfe Dritter bedient. Insbesondere habe ich wörtlich oder sinngemäß aus anderen Werken übernommene Inhalte als solche kenntlich gemacht
3. Ich habe nicht die Hilfe einer kommerziellen Promotionsvermittlung oder Beratung in Anspruch genommen.
4. Die Bedeutung der eidesstattlichen Versicherung und der strafrechtlichen Folgen einer unrichtigen oder unvollständigen eidesstattlichen Versicherung sind mir bekannt.

Die Richtigkeit der vorstehenden Erklärung bestätige ich: Ich versichere an Eides Statt, dass ich nach bestem Wissen die reine Wahrheit erklärt und nichts verschwiegen habe.

_____ _____

Ort und Datum Unterschrift

Lebenslauf:

Berufliche Erfahrung und akademische Ausbildung

09/2014-Heute	Software Engineer Life Science Analytics bei der accantec consulting AG
02/2014-08/2014	Wissenschaftlicher Mittarbeiter, Universität Hohenheim, Institut für Lebensmittelwissenschaften und Biotechnologie, Fachgebiet: Prozessanalytik und Getreidetechnologie.
02/2011–01/2014	Promotionsstudent, Universität Hohenheim, Institut für Lebensmittelwissenschaften und Biotechnologie, Fachgebiet: Prozessanalytik und Getreidetechnologie.
10/2009-01/2011	Promotionsstudent, Universität Hannover, Institut für Technische Chemie Arbeitskreis: Bioprozessanalytik und -automation, Chemometrie, Bioinformatik
10/2004-09/2009	Studium: Bachelor und Master Life Science, Universität Hannover Spezialisierung im Master: Bioprozesstechnik und Bioinformatik.
	Masterarbeit: „Erstellung einer Auswertungssoftware für einen Ultraschallresonator“, Abschlussnote: Exzellent
	Bachelorarbeit: „Auswertung einer geregelten E.coli Kultivierung mit sehr geringer Substratkonzentration“, Abschlussnote: Gut

Veröffentlichungen

M. Stanke and B. Hitzmann (2013), Automatic Control of Bioprocesses, Measurement, Monitoring, Modelling and Control of Bioprocesses. C.-F. Mandenius and N. J. Titchener-Hooker, Springer Berlin Heidelberg. 132: 35-63.

M. Stanke, P. Lindner, S. Holz, B. Hitzmann (2013), Automated sonic velocity calculation based on ultrasonic resonator measurements for on-line process monitoring, Sensors and Actuators A: Physical, 198: 69-74.

M. Stanke, V. Zettel, S. Schütze, B. Hitzmann (2014), Measurement and mathematical modeling of the relative volume of wheat dough during proofing, Journal of Food Engineering, 131: 58-64

F.Hecker, M. Stanke, T. Becker, B. Hitzmann (2014), Application of a modified GA, ACO and a random search procedure to solve the production scheduling of a case study bakery, Expert Systems with Applications, 41(13):5882-5891

S. Holz, M. Stanke, M. Hartlep, W. Peters, M. Lehmann, P. Lindner, B. Hitzmann, S. Beutel, T. Scheper, R. Winter (05/2010) Online-Analyse von Proteinen mittels Ultraschall; CIT-journal 2010, 82, No. 9, S. 1407

Vorträge

M. Stanke, Anwendbarkeit der Semi- C64 Methode für nicht normalverteilte Prozessdaten für Six-Sigma,
JMP User Group Treffen, Schott 2015.

M. Stanke, Optimale Parameterbestimmung von Nicht-Linearen Funktionen,
JMP User Group Treffen, Procter & Gamble 2016.

M. Stanke, Application of the SEMI C64 algorithm to calculate the control limit for non-normal distributed process data using JMP Scripting, JMP Discovery Summit, Brüssel 2017.